8-2021

The Application of Laser Induced Breakdown Spectroscopy to Molten Salt Corrosion

William S. Ponder
wponder@utk.edu

To the Graduate Council:

I am submitting herewith a thesis written by William S. Ponder entitled "The Application of Laser Induced Breakdown Spectroscopy to Molten Salt Corrosion." I have examined the final electronic copy of this thesis for form and content and recommend that it be accepted in partial fulfillment of the requirements for the degree of Master of Science, with a major in Nuclear Engineering.

Steven J Zinkle, Major Professor

We have read this thesis and recommend its acceptance:

Accepted for the Council:
Dixie L. Thompson

Vice Provost and Dean of the Graduate School

(Original signatures are on file with official student records.)

The Application of Laser Induced Breakdown Spectroscopy to Molten Salt Corrosion

A Thesis Presented for the

Master of Science

Degree

The University of Tennessee, Knoxville

William Ponder

August 2021

ACKNOWLEDGEMENTS

Thank you to my mother and father for allowing me to be here.

Thank you to my brother for always being willing to entertain strange ideas no matter when I call him.

Thank you to Marc for being a good friend through good and bad.

Thank you to Steve for providing me the opportunity to pursue an advanced degree at UTK.

Thank you to Stephen for taking a chance on an un-proven student.

Thank you to Kristian for providing mentorship well beyond what was required of him.

Thank you to the many people of the Zinkle group who have always provided excellent conversation and assistance as I have needed.

Thank you to my friends from the UTK Clay Target Team who have provided an important outlet when my patience has run out.

Thank you to those brothers who have called me to always aim higher in my pursuits.

ABSTRACT

Molten salt reactors (MSRs) have a plethora of advantages over light water reactors. They operate at more favorable conditions for power generation and accident conditions. These conditions lead to problems with corrosion. Monitoring of this corrosion will be required for a MSR when built. Laser Induced Breakdown Spectroscopy (LIBS) is an excellent tool for this application, as it can be done with minimal sample preparation and without having to complete the more complex sample preparation required for EDS. This work will demonstrate the utility of LIBS in showing similar features as EDS such that an understanding of the corrosion seen in a material is achieved through LIBS.

TABLE OF CONTENTS

LIST OF FIGURES

CHAPTER ONE INTRODUCTION

Brief overview of MSRs and their importance

Clean, carbon-free energy is important for the continued advancement of humanity. Nuclear energy is an excellent option to that end. Nuclear energy has many advantages, particularly the energy density of fissile material allows for small footprints compared to renewable energy. Nuclear reactor designs outside of current commercial plants exist and offer novel features that could be of further benefit in producing cheap, carbon free electricity. Of these existing designs, Molten salt reactors have a host of advantages worth discussing. However it also has a number of challenges that must be addressed. This work will discuss some of the materials and chemical challenges faced by MSRs, as well as provide some insight into these systems using the LIBS analysis technique.

Molten Salt Reactors are an important technology that could be transformative to electricity generation in the near term. Molten salt reactors are considered to be a more attractive option than Light water reactors (LWRs), which are a technology that is already quite good at producing safe and clean energy. Simplicity and physics-based behavior are the backbone of the safety of the MSR design. Many of the additional benefits past simple safety come from the more complex chemistry that is both the greatest benefit and challenge of the MSR. Amongst the considerable benefits of the MSR design are low pressure, high temperature operation, inherent safety, increased fuel utilization and the potential to use fertile material to fuel the reactor. Technical challenges in the areas of materials corrosion, chemistry control, and proliferation concern need to be dealt with before a commercial version of the MSR could be viable. Upon successful resolution of the few challenges, MSRs offer a technology that could help to produce large amounts of carbon-free energy with significantly more rapid deployment than fusion.

LWRs rely on high pressure to keep water a liquid. This is a problem, as it means there is a large driving force that might distribute radionuclides in the case of an accident in an

LWR and when pressure is lost in an accident. This high pressure also leads to requiring thick piping, pressure vessels, and materials capable of withstanding these pressures, all which increases cost and makes maintenance of LWRs difficult. By lowering the pressures involved, the molten salt reactor design does not require a massive pressure vessel, nor do the pipes containing coolant need to contain hundreds of atmospheres of pressure. Similarly, the threat of distributing contamination in the event of an accident is reduced since there is no pressure gradient that could disperse material. Finally, molten salt does not have the same possibility of the coolant becoming gaseous in accidents that water has. This is of benefit, as it means even in accidents, coolant should be present. Lowering pressure is an important benefit of the MSR design.

The high temperature operation of MSRs has one simple advantage. To get one watt of electricity from a steam turbine requires about 3 watts of heat (rough assumption). By operating at higher temperatures, MSRs are more thermodynamically efficient and will require less fuel to produce the same electrical output. Rather than the 33% thermal efficiency number of typical turbines in current power plants, molten salt will likely have thermal efficiencies closer to 45%[1]. In other words, MSRs are a more fuel-efficient design than LWRs; producing the same amount of electricity in a MSR uses less fissile material than what a LWR would require.

A third benefit of the MSR is its inherent safety. There are various methods that achieve this; however, none are quite as simple as the freeze plug concept. The freeze plug is a small section of piping that requires constant cooling to keep the reactor coolant contained within the normal vessel by solidifying salt within a drain tube. In the event of an event where power is lost to the reactor, cooling of the freeze plug is lost, and the plug melts. This plug melting allows the volume of the reactor to drain into tanks designed to stop any ongoing fission reactions, and to cool the salt. This design feature is highly important, as it makes the MSR reactor “walk away safe,” meaning that no human input is needed to prevent catastrophic consequences from even the worst accidents.

Molten salt reactors offer the opportunity to actively separate fission products during operation. This is a huge advantage, as it allows for the breeding of fuel from Th, and decreases the amount of fission products in the salt. During normal operations, this means that Xe-135, Gd-155, Gd-157, Sm-149 and other neutron poisons are removed from the core, increasing the neutron utilization of the reactor. In other words, less fissile material is needed to sustain a chain reaction. Online processing of fuel offers another potential benefit of separating radioactive fission products that might be used for medicine, imaging, or other applications as needed. The fissioning of material leads to the production of many useful radioisotopes. For example, Mo-99 is produced from the fission of U-235. This is a highly important radioisotope, as it decays to Tc-99m which is used for medical imaging. Many examples of this exist, providing the opportunity for a MSR design to produce radioisotopes as an additional benefit.

The MSR is not a single reactor design, but rather a classification of design. Just as a car and a bike are both vehicles, the MSRE, ARE, and paper reactors are all MSRs but are radically different in form. Different designs of MSRs may be optimized for differing performance, some may breed fuel, some may use a fast spectrum to limit waste production, and some may be used to produce radionuclides for medical applications. Molten salt reactors offer the option of using Th-232 to breed U-233 for fuel, avoiding the production of Pu, and limiting the production of transuranic elements. This is important, as much of the long-lived radioisotopes in nuclear waste are transuranic and eliminating their production means that waste will be shorter lived and produce less heat. Breeding fuel and burning waste are important potential uses of future MSRs that the various designs proposed can take advantage of. The lack of a single design is a strength and challenge for MSR implementation. There is utility in being able to attribute every benefit as a selling point, however this is a problem when discussing MSRs. The lack of a standard design creates a great challenge when discussing MSRs, there is no single MSR or MSR model that represents everything, and thus there is not a standard by which corrosion, chemistry, performance, and other characteristics of a MSR may be measured

or discussed. For example, the same reactor cannot breed fuel from Th-232 and burn large amounts of LWR waste, but both are discussed as potential benefits of the MSR design, and a simple reading of the benefits of MSRs might mislead the reader into thinking that every espoused benefit of the MSR would be present in all MSR designs.

Problems exist with the MSR design. There has not been a MSR built in over half of a century, and that experiment was limited in power and operational time. The hands-on knowledge of running a nuclear reactor using molten salt now exist mostly on paper rather than in the minds of people. Technical reports are all that remains of the non-scientific knowledge of building MSRs. There are undoubtedly things that were learned about molten salt systems during their operation that have been lost to time.

Considerable corrosion challenges exist for the MSR. Hastelloy N worked for the MSRE. However, it is highly expensive, and it is not code rated meaning it would not be permissible to build a commercial system using it. Hastelloy N also had a problem with Te induced cracking. While later studies found solutions to the Te induced cracking, there are likely other materials challenges that have not been fully addressed. For the MSRE, the chemistry control that ensured that corrosion was minimal was manageable but difficult. Specific measurements of the redox state of the salt were taken prevent corrosion problems at set intervals. Constantly measuring and adjusting of a system is expensive and complicated, facts that would limit the implementation of a MSR. Finally, Modern corrosion studies have found that impurities in salt will increase corrosion. High rates of fission producing a wide spectrum of elements is likely to be problematic for introducing impurities and affecting corrosion, the previously mentioned Te cracking was found, it might be that other problems would arise. Without running further test reactors, there is uncertainty about what fission products might do to a MSR.

MSRs present a potential proliferation risk in some situations. Any of the breeding fuel cycles have the possibility of separating materials that could be directly used in weapons. Similarly, the ARE and MSRE designs used uranium enrichments higher than what is

allowable under the current licensing framework due to concerns of proliferation. While the goal of making a MSR to produce cheap, carbon free energy is good, it must not come into conflict with the goal of preventing the proliferation of nuclear materials.

The MSR technology has many benefits that it offers in producing the energy needed for the world. The high safety and efficiency along with the benefit of breeding fuel are all fantastic. Technical challenges remain in the way of the MSR being implemented.

Brief introduction to LIBS

Laser Induced Breakdown Spectroscopy (LIBS) is a technique used to determine the composition of a sample. LIBS operates by firing a high-power laser at a material, depositing a large amount of energy as heat to the material, which causes it to turn into plasma. A plasma is a state of matter similar to gas, but where electrons are not bound to atoms and are free to move. As the volume of created plasma cools, the electrons that were removed from the atoms that make up the plasma return to their original position orbiting the atom. This return of electrons results in the emission of photons (light) with specific energies based on how the electron returned to orbiting the atom. This characteristic photon energy specifies what elements are present. After flashing a small volume of material to plasma, the process is repeated, and the laser is fired again at the same fixed point. The emission spectra of this volume of material is recorded and the laser is repeatedly fired. This process repeats until the laser has completed "burning" through the depth of interest. Control of this depth of interest is achieved by changing the laser power, laser beam shaping, and beam size. Laser power changes emissions by producing hotter or cooler plasmas based on the energy input to the system. Adjusting plasma temperatures allows for more or less activation of certain emission lines, a feature that can enable more selective analysis of elements. Beam shaping matters as it determines what the volume of material flashed to plasma is shaped like. The most common beam shapes for LIBS are Gaussian power distribution and top hat (flat top) power distribution. Finally, spot size can be chosen to help include more or less of the

localized features or simplify things for bulk analysis. Often LIBS is repeated at multiple positions on a sample to ensure that many representative areas are analyzed. This process allows for both homogenized analysis and comparison from one location to another where differing features may be analyzed. A final important detail of LIBS characterization is that of gate delay. The collection of a LIBS spectra begins with the pulsing of a laser. This begins a clock in the spectrometer that will measure the emitted light from the produced plasma. The delay between when the laser is fired and when the spectrometer begins to collect data is an important parameter in determining the behavior of the system, as it determines the plasma temperature. Shorter gate delays have extra noise from black body radiation, while longer gate delays have less signal.

Producing accurate quantification for the amount of an element present in a single LIBS spectrum is a complicated task. Within a spectrum, there will be a background continuum superimposed with the spectral peaks. This background level of photons is produced by black body radiation of the plasma as it cools from high temperatures. Next, there will be emission peaks from the cover gas which will be superheated by the laser when a measurement is done. These peaks need to be ignored or removed depending on the analysis. Finally, known peaks based on the elements expected should be seen. Every emission peak has a relative intensity which is known for most elements. The relative intensity is an important concept, as some emissions will be quite common and result in a clear signal, while other emissions will be rare and result in minimal or no peak. There is also an important consideration of how hot the plasma is. Variations occur in laser power that can result in a hotter or cooler plasma that will produce different peaks. A hotter plasma will have more energy and will likely produce more uncommon peaks. Similarly, a cool plasma might not produce some expected emissions.

LIBS is technically a destructive analysis technique, however it often considered as non-destructive as very small pieces of material can be used for analysis. It is an important caveat that LIBS does destroy at least some of a sample, which can be a problem for small samples that are expensive and complex to produce.

Applying LIBS to molten salt systems should be able to provide analysis of several features of corrosion and material degradation. Molten salt corrosion will lead to removal of the least noble metal from the alloy, metal or material exposed, meaning there will be a depleted region of some element observed by LIBS. LIBS will similarly be able to detect if there is salt trapped in openings, pores, or cracks. It is possible that depletion of elements along grain boundaries that have been attacked by molten salt can be detected using LIBS. Additionally, LIBS will be able to see if there are any other elements present from the salt that would suggest the exchange of metal from the alloy for metal from salt to create corrosion. For example, we may detect small amounts of Mg that would indicate that Mg from the salt was reduced when Cr was oxidized. This might indicate that there are possible reactions that are not well mapped with the current understanding of the thermodynamics of the salt-metal system.

MSR History

History of ARE

Following the second world war where nuclear energy had been demonstrated to devastating effect, the US Army Air Forces began to seek out a solution for a nuclear-powered aircraft. Sustained supersonic flight was the goal of the Aircraft Nuclear Propulsion program. With high energy densities, nuclear was considered as a power source for such an aircraft. The reactor they built was known as the Aircraft Reactor Experiment (ARE). This program resulted in the building of the first molten salt reactor, wherein a $NaF\text{-}ZrF_4\text{-}UF_4$ salt was circulated through a BeO moderator. The metal used for the construction was an Inconel high Ni content alloy. The ARE was built and operated at a 3 MW power. The thermal gradient across the core was 355°F (197°C), and the highest temperature within the reactor was 1620°F (882°C). The ARE operated for a total of 4 days from November 8 to 12, 1954. The technical reports from the ARE are available [2, 3]. These reports fully detail the design, construction, operation, and post

experiment examination of the ARE. The project was reported as a success and set the groundwork for the MSRE and future MSR concepts.

The work of the ARE is highly relevant, as it was the first MSR ever constructed. This work successfully demonstrated that molten salt reactors are possible to build and operate. Amongst the important lessons from the ARE were that the Inconel that was used for the reactor vessel and containment was not compatible with molten salt[3]. Earlier corrosion testing has shown Inconel to corrode more than stainless steels, however its high-temperature strength, ability to be fabricated, and availability made it the choice of material for the ARE.

The end of ANP occurred for several reasons, however the primary reason was the development of Intercontinental Ballistic Missiles. Their development eliminated the need for sustained supersonic flight and an energy source that could power it. This left the molten salt technology in somewhat of void until civilian power was suggested as an application of molten salt. The ARE left the legacy that would enable the MSRE and spark the interest in molten salt technology.

History of MSRE

A decade after the ARE, a second demonstration of the molten salt reactor concept was designed, built, and operated from 1965 to 1969. It operated at up to 7.4 MWt and had a hot leg temperature of 650° C. Initially the MSRE ran on enriched U-235 as its fissile fuel, however it later was operated using U-233 as the fissile material, demonstrating the possibility of running such a reactor fuel cycle. The additional utility in operating a nuclear reactor using U-233 is enabling the possibility of breeding fuel from Th-232.

The salt used in the MSRE was $LiF\text{-}BeF_2\text{-}UF_4$. The materials that were in contact with the salt were all graphite or Hastelloy-N, a special alloy developed specifically for work with molten salts. Hastelloy N has a composition 7% Cr, 16% Mo, <4% Fe, <1% Si, Mn, V, Co, Cu, W, Al, Ti, and balance (~71%) Ni by weight percent. The thermodynamics

and design are discussed in greater detail for this alloy in following sections, however it was found to be a good choice for work in molten salts due to low Cr content. Of the alloy constituents, Cr would be selectively removed first, leaving the majority of the metal in place. The MSRE design relied on graphite as a moderator. Graphite was found to be compatible with molten salt so long as it had small pores.

Corrosion in the MSRE was found to be minimal, with Cr content in the salt measured at 85 ppm at the end of the first major series of operation. This was equated with a 0.2 mm or less loss of structural material on any of the exposed surfaces. It is important to note that the MSRE had a high degree of control on their salt chemistry, often sampling and measuring the amount of U(III) against the amount of U(IV). This ratio was held constant such that metal would not be reduced and plate out anywhere in the system, and that structural metals would not be oxidized. This is highly important as it is likely why the MSRE did not experience significant corrosion whereas some experiments with molten salt experience high corrosion rates.

The technical issues from the MSRE are reported and further discussed in the work [4]. Amongst the problems reported are structural material embrittlement, limited graphite lifetime, molten salt chemistry, noble metal plate out, tritium management, power fluctuations, and design maturity. All of these were addressed in post MSRE works to varying degrees. Embrittlement of Hastelloy N was attributed to Te. Te occurs in molten salt systems as a fission product, and it was found that a Nickel-Telluride intermetallic compound was formed that led to significant cracking of the Hastelloy N used to contain salt. Significant work followed at ORNL developing a modified Hastelloy N that would be resistant to this cracking. Experiments were initially done as capsules and then loops to confirm the behavior of additions to the alloy. This was found to be a diffusive process, as the depth to which Te was present was found to be proportional to the square root of the exposure time. The mechanism suggested for the embrittlement of Hastelloy N was the formation of Ni_3Te_2. It was eventually found that Te cracking of Hastelloy N could be stopped by adding a small (~1-2%) addition of Nb to the alloy[5-7].

A huge number of technical reports were generated for and from the MSRE, and while all provide useful information for MSR research and design, a selected few are included as sources. These include reports on the characterization of corrosion samples post-experiment [8-11], general design [12, 13], and chemistry [14].

The MSRE was a significantly longer experiment than the ARE and thus had more challenges but resulted in greater knowledge. Many proposed modern reactors suggest using the same salt for the same reasons; greater data is available for the FLiBe mixture than any other salt, and its neutronic properties are ideal. The idea of a freeze plug has become universal based on its inclusion in the MSRE design. The MSRE was considered a success in its plans, as it demonstrated the technology and helped to expand knowledge on the MSR design type.

History of MSBR and paper MSRs

Following the MSRE, a further demonstration of the MSR technology was planned. The Molten Salt Breeder Reactor was one of a series of following designs that came from the interest and work done in the MSRE. The MSBR was proposed as a larger reactor on the order of several hundred MW power [15]. The intention was to use the lessons learned from the MSRE to develop a full scale MSR that could provide civilian nuclear power[16]. The MSBR design was to use a similar salt, and the same alloy, save the Nb addition to Hastelloy N and the addition of Th to the salt [4]. The MSBR proposed breeding fuel from Th. The advantages of breeding Th to U-233 are reduced waste, no enrichment requirement, and greater fuel availability. The MSBR would require online chemical separation as a part of its operation. The neutron capture of Th-232 produces Th-233 which decays rapidly to Pa-233. This Pa-233 needs to be chemically separated to prevent further conversion. Once captured, Pa-233 is allowed to decay to U-233, a fissile fuel. This process of continuously separating Pa had been demonstrated on a lab scale, however the MSRE only had chemical separations at intervals rather than continuously[17]. The integration of an online separation of fission products was of

concern and is one of the technical challenges that remains today. Funding for nuclear reactor designs was limited, and for a myriad of political and scientific reasons, the Atomic Energy Commission chose to pursue liquid metal fast reactors. A final few reports of importance were generated from ORNL on the potential of the MSR design following this decision. Of particular importance are [7], and [18].

Other MSR concepts exist in papers particularly from ORNL. The denatured MSR and FHR are amongst these paper reactors proposed. Each has benefits to its design. The Denatured MSR (DMSR) is designed for particular concerns of proliferation that MSRs generally present[19]. The high enrichment and requirement of continuous chemical separation is of concern, and the DMSR Materials accountability is difficult in MSRs, the DMSR works to fix this by designing with the limits of 5% enriched U-235 fuel, making the theft of fuel less of a proliferation risk. Similarly, the DMSR works to solve the problem of producing Pu by limiting the separations processes needed during operation. Many potential MSR designs can be made with a host of benefits, however they must all deal with the suite of problems that molten salt presents from a chemistry and materials perspective.

Current MSR designs

After several decades of limited interest, there is renewed interest in molten salt reactor designs primarily from an industrial perspective and several are worth mentioning. Kairos Power is one company with a MSR design, relying on multiple technologies, they plan on loading TRISO fuel pellets in to a LiF-BeF_2 (FLiBe) salt, having a secondary salt heat transfer loop, and finally using that heat in a steam generator to produce the steam to run a thermal cycle. Their planned output is 140 MWe. Peak salt temperature is planned to be 650° C. Fuel loading is planned as 19.75% U-235 content.

TerraPower has several nuclear reactor designs, including the Molten Chloride Fast Reactor. The MCFR is a MSR that is designed to use a chloride salt as a coolant. This is a departure from other designs, and may require the isotopic separation of Cl-35 and Cl-37.

The benefits and problems of using Cl based salts will be discussed in a following chapter.

FLiBe energy is another company invested in producing a MSR for the commercial market. Their specific specialty is that their reactor design would use Th as a fertile fuel rather than relying on U as the fuel for the reactor. Limited information is available on the physical properties of their reactor design.

The purpose of mentioning all of these reactors is to demonstrate the commercial interest in the technology. Other designs have been proposed with different goals of using Th or U for Fueling, Cl or F salts, and a whole host of other goals that would be beneficial to operation of a MSR. Renewed MSR interest is important, and is important justification for this work, and the other novel works that are occurring in molten salt science.

CHAPTER TWO - LITERATURE REVIEW

Molten Salt

Introduction

Molten Salt is a complex topic that merits discussion. From the ground up, it is important to understand why certain elements are selected to make a salt and why other elements are not. It is similarly important to know why some materials work better as containers for molten salts. Finally, the thermodynamics of these selections are important to know and understand. The resulting interaction of the selected salt and metal will show some general trends in what elements of the structural metal are attacked. The severity of the attack faced by the metal is in large part controlled by the impurities seen in the salt. Chloride salts appear to have more impurities and have more complex chemistry. All this chemistry is controlled with metallic additions that keep the redox state of the salt at a proper set point. Understanding all this requires testing, particularly thermal convection loops. Finally, the reported values from testing need to be depth of attack rather than mass loss to correctly identify the amount of material that no longer is structurally sound.

Salt selection Requirements

The anions and cations that go into making a molten salt are critical and differ vastly based on application. Generally physical properties and nuclear properties must be balanced to produce an ideal salt. The requirements of having low enough temperatures for materials to survive means that the salts used will need to be mixtures, preferably eutectic mixtures, of two salts. Generally due to thermodynamic concerns, the middle of the periodic table is avoided due to having low energy of formation as halides. This means that the structural materials would be able to be more easily reacted by the less tightly bound halides found with salts from these metals. This leaves the alkali metals and the alkaline earth metals for consideration as salt materials. There are exceptions to this,

primarily Zr. Salt cations can be selected from most of the alkali and alkaline metals with concern mostly given to producing ideal physical and nuclear properties.

An important limitation of any salt mixture intended for reactor use is that it must have U, Zr, or another cation that is able to have multiple oxidation states in the salt. Cations with multiple oxidation states are able to act as buffers in the event that there is a shift in redox chemistry in the reactor. In the MSRE, the salt was primarily LiF and BeF_2, 65 and 29 molar percent respectively, however the salt also contained 5 mole percent ZrF_4 and 1 percent UF_4. These salts provided a buffer such that were the chemistry of the salt to become more oxidizing, the small amount of UF_3 in the salt would become oxidized before structural metals. A similar change could happen in the Zr should the chemistry dictated that reaction was favored. If the salt became reducing, UF_4 would be reduced to UF_3 before fission products or U metal was reduced out of solution in the salt. For these chemical reasons, it is essential to include cations with multiple oxidation states in molten salts.

Many concepts from MSRs use FLiBe salt. FLiBe salt is a mixture of LiF and BeF_2 with approximately 2 parts LiF to 1-part BeF_2. FLiBe salt is an ideal choice from a nuclear properties perspective, particularly FLiBe enriched in ^{7}Li, due to its low absorption of neutrons. For reactors using once through fueling this concern is not significant, and a wide variety of cations may be used. K for example has a neutron cross section that would prevent it from being used in a thermal breeder reactor, however a once through fuel cycle could be completed using a salt with K. As the average neutron energies of the designed reactor change, so to do the materials that a salt can use and sustain breeding operations. To breed with fast neutrons, most elements may be used. To breed with intermediate spectra, only, ^{7}Li, Be, Na, Mg, Al, Zr, Ca, Rb, and Ce may be considered as cations. ^{35}Cl must be removed from a Cl salt to breed fuel in a reactor, as it has a high neutron absorption cross section. To breed fuel with a thermal spectrum, FLiBe with ^{7}Li provides the needed performance. Knowing all of this, the most common salts are FLiBe, FLiNaK, KCl-$MgCl_2$, and NaCl-$MgCl_2$. Other salts exist, particular for applications in

pyroprocessing of spent nuclear fuel. The 2006 paper *Assessment of Candidate Molten Salt Coolants for the Advanced High-Temperature Reactor(AHTR) [20]* has a good assessment and discussion of the reasons why some elements may not be used for a salt while others are preferred. The discussion covers physical, chemical and nuclear properties, and why a contain salt might be chosen as a balance of these properties.

An important note is that non-halide salts are not viable for MSR applications for several reasons. First, complex salts such as nitrates and carbonates break down under radiation and would not provide good performance. Secondly, these systems often have materials challenges at least as difficult as halide systems. Finally, these systems do not allow for dissolving enough fissile material to sustain a reaction. For these reasons, MSR designs will always use halide salts.

Salt facing metal selection for molten salt applications

The materials typically proposed for use in high temperature molten salt are graphite and metals. Graphite is inert in molten salt so long as the porosity of the graphite is small and does not allow significant trapping and interaction with salt. However, graphite is not a focus of this work (where traditional structural alloys are required due to design restrictions) and will not be discussed further.

Selection of metals for molten salt has been a highly debated topic since the ARE. The ARE used Inconel alloy as it was thought to be sufficiently resistant to corrosion in molten salt and had better high temperature strength than stainless steels at the time. Problems were found with high corrosion rates using Inconel, and for the next decade, considerable work was done to develop Hastelloy N, a nickel-base alloy tailored to withstand the environments faced in FLiBe salt. Hastelloy N is resistant to molten salt corrosion due to several features. First, the high Ni content means that much of the alloy is inert in the salt. The relatively low Cr content (7%) is attacked but is sufficiently low to saturate the oxidizing conditions faced by the salt in static reactions without oxidizing other metals. Mo is used to strengthen the alloy and add further noble metals to the alloy.

Hastelloy N has many beneficial properties in molten salt including corrosion resistance and adequate high temperature strength. However, Hastelloy N is relatively costly and it embrittled during operation in the MSRE. Through the work conducted following MSRE, grain boundary embrittlement was found to be associated with Te fission products. This problem appears to be solved by the addition of Nb into the standard Hastelloy N alloy. Other variations of Hastelloy N exist with goals of improving performance. Price is a problem for the Hastelloy N alloy, as its high Ni content is expensive. Hastelloy N is also not used in any other industry, and thus test coupons and later fabrications are not widely available. Another problem for Hastelloy N is the potential for neutron irradiation produced He bubbles. The formation of He through the two step (n,a) reaction may lead to material problems as seen in irradiation of other high Ni content alloys[21]. The work dealing with Te cracking following the MSRE appeared to solve the embrittlement problem; however it is possible the production of He bubbles embrittling metals may have been a contributing factor that has not been sufficiently well studied in the degradation of MSR materials. Finally, Hastelloy N is not ASME code qualified, meaning before anything could be built using Hastelloy N it would need to be rated per ASME coding specifications.

The expense and limited availability of Hastelloy has led some to suggest using 316 stainless steel for molten salt. 316 is a steel alloy, and thus more data already exists, it is code qualified, piping and plates are available, and 316 is significantly cheaper than Hastelloy N. These benefits come at the cost of some corrosion resistance. 316 is more susceptible to corrosion than Ni alloys due to higher Cr content, and being a majority Fe-based alloy, which is more prone to corrode due to being more chemically preferred as a halide compared to Ni. There is work from ORNL that suggests that in high purity molten salt, there is not a significant difference between corrosion in 316 and Hastelloy N for temperatures up to ~650° C. ORNL has also operated a molten salt loop using 316 SS and FLiBe salt demonstrating that 316 can successfully withstand loop conditions[22]. It is also worth noting that there has not been work done studying the potential interaction

of Te and 316H. 316H has a high Ni content making it possible that it would see the same issue as Hastelloy N in forming Nickel Telluride at grain boundaries. Research has not been done to study this however, so this all must be taken as speculation.

Generally the alloys that work for molten salt have several things in common. They rely on having a sacrificial component that reacts until chemical equilibrium is achieved. This typically means that Cr is included. They have good high temperature strength, and they must be able to be machined into whatever shape is needed. Generally, the alloys considered are Hastelloy N and 316H, however between these two alloys more molten salt data exists with Hastelloy, (particularly more flowing tests) and it should be considered as superior.

Molten Salt Thermodynamics

Molten Salt Has a complex set of chemical interactions that control its behavior. The reactions that describe salt chemistry are the fluorination and chlorination of metals. The best tool to understand this is an Ellingham diagram describing these reversible chemical reactions. An Ellingham diagram reports the change in free energy (or one of its derivatives) as a function of temperature for a chemical reaction or set of chemical reactions. Ellingham diagrams for common salt cations and structural metal alloys are presented in figure 2-1. The alkali metals are highly reactive with the halides and thus have large free energies of formation. The alkali earth metals are less reactive with halides, but generally have significant free energies of formation. The transition metals are not highly predictable in their interactions with molten salt. Some elements are highly favored to be metals, while others are favored to be salt. What this all means is that if there is Li and Fe in the presence of Cl, the Li is significantly more likely to react, and even should the Fe be oxidized, if contacted the Li would reduce the Fe and become oxidized and reduce the iron oxide to metal.

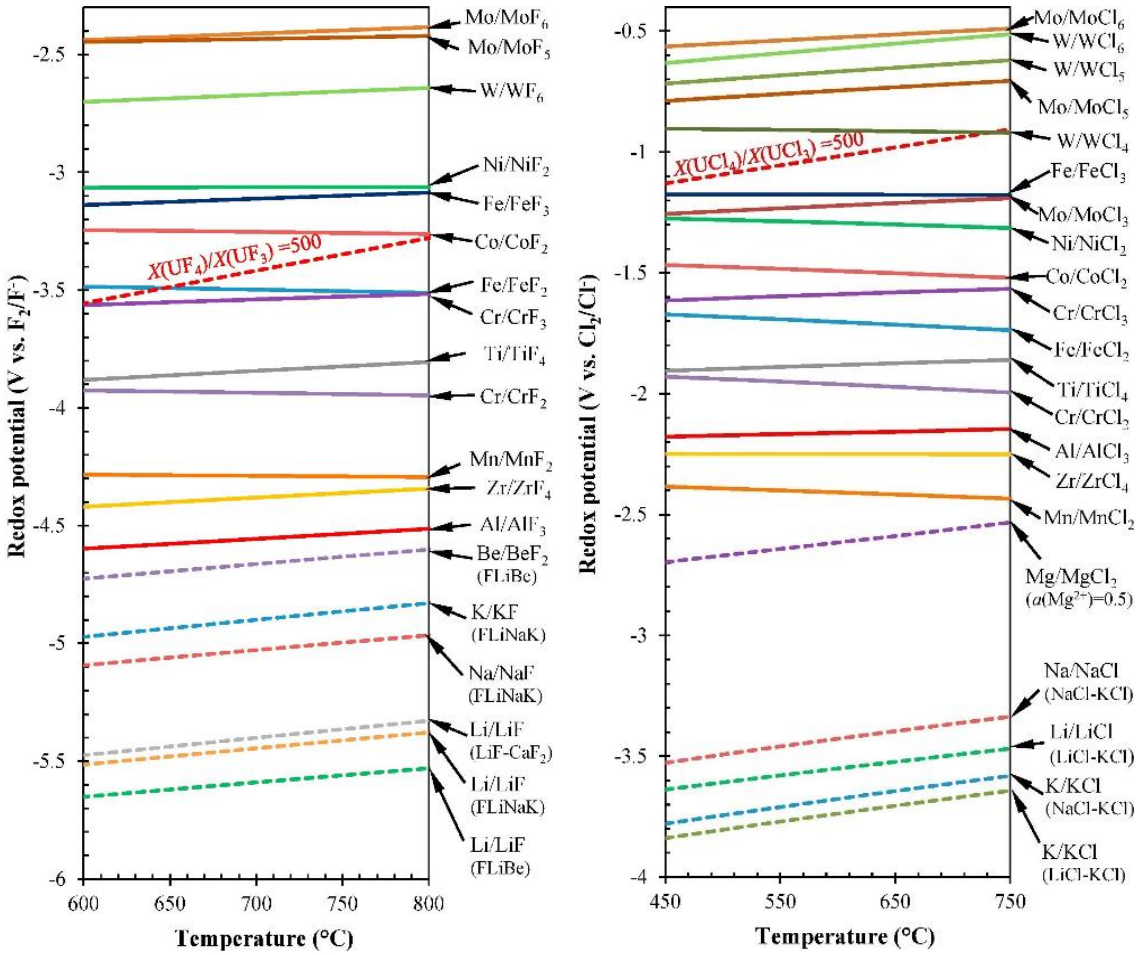

Figure 2-1: Ellingham Diagram of Fluorides and Chlorides

Ellingham diagrams for Fluorine and Chlorine are presented above. Elements at the bottom are most stable as salt while elements at the top are more stable as metals. These charts are of great importance, as they predict exactly what elements will be oxidized first, and what metals will be stable in molten salt. [23]

All of these reactions are equilibrium reactions, and not all of the metal in the system will oxidize. Instead, some will remain metal while most would be oxidized, satisfying the reaction constant for the equilibrium reaction. The implication of this is that adding some metals will have little effect on what occurs in the molten salt, but others would greatly affect the chemistry of the system. For example, if a huge amount of Na metal was dumped in a NaCl-$MgCl_2$ salt, it would be possible to produce Mg metal. This would generally mean that any Cl in the system would react with the Mg metal in the system and would prevent the possibility of oxidizing structural metals. The problem this creates is that of reducing fissile material and fission products out of the salt in a reactor with circulating fissile material. For this reason, high control is needed of the state of the chemistry in a MSR. The MSRE did this by monitoring the oxidation state of the U in the system and maintaining a balance of U(III) and U(IV). If that balance was wrong, Be metal could be added to reduce some of the U(IV) and make more U(III). If U(IV) was in excess, HF could be used to react with excess U(III) to produce U(IV). This delicate balance worked for the MSRE chemistry control to keep corrosion low by not favoring the oxidation of Cr, and by favoring the oxidation of U and fission products. This balance is one of the most important portions of any molten salt system, as being excessively oxidizing would result in high corrosion rates, while being highly reducing would plug pipes and fix contamination and fissile material.

The paper that best discusses the thermodynamics is [23]. In that paper, the author discusses the corrosion of molten salt systems covering thermodynamics, impurities, electrochemistry and how redox control can be used to limit the corrosion seen.

A report following the MSRE and concluding work was completed by C. F. Baes [24]. In this report, the understanding of the thermodynamics that was developed in the MSRE and ORNL testing programs through the early 1970s is reported. Discussion in this report covers several important topics that are a good introduction to the fundamentals of molten salt corrosion. The topics of using HF to limit oxide impurities, the oxidation of structural metals, the chemical suspension of actinides and lanthanides, the chemistry of

the fuel, the impact of having fission occurring, and tellurium induced cracking are all reported in this classic journal article.

Least noble metal oxidation

As previously discussed, the reaction of the halide from a molten salt with any metallic elements that might be exposed to it are highly favored. If there were an excess of salt to provide free halide anions, any piece of metal would be reacted. Halide anions are supplied through the decomposition of salt at an equilibrium rate as the production of any salt is an equilibrium reaction. This reaction produces some amount of free halide so long as there is not sufficient halide present to balance the reaction. This formed halide is what reacts with exposed metal. Were a sufficiently large amount of salt exposed to a small specimen, the specimen would be dissolved. The opposite case is also possible, where a large metal sample would not allow for the saturation of the chemical reactions occurring at the sample surface. More salt present would mean more halide anions would be available to oxidize metal and result in more metal being reacted to salt. All that being said, the limited availability of free halide results in selective oxidation of the least noble metals in an alloy, as the little bit of free halide is most favorably reacted with those alloy constituents that have the greatest free energy of formation. This causes the process of least noble metal oxidation. A simple example of least noble metal oxidation would be Cr and Ni mixtures. It is favored to form $CrHa_2$ rather than $NiHa_2$ (where Ha is a halide anion) based on the thermodynamics of the Cr having a greater free energy of formation. With the available halide in the salt reacting with the least noble member of the metal exposed, there are two general possibilities for what occurs. In one possibility, there is an excess of least noble metal at the sample surface, and the reaction slows based on limited availability of halide anions from the salt. This attack likely forms the more uniform sections of molten salt corrosion. The second possibility is that the rate limiting step for the reaction is the loss of the metal from an alloy. If there is a small amount of least noble metal in the alloy, it is possible that all the least noble metal that is in contact with the salt

at the interface between metal and salt will react, leaving the more noble constituents of the alloy behind. More of the least noble metal is available in the portion of the alloy that is not in contact with the salt, however it must be moved to the salt-metal interface. Molten salt systems are at high temperature (>500 C) where thermal diffusion is generally able to transport more of the least noble metal from the bulk of the alloy to the salt-metal interface. Grain boundaries act as locations where there is a greater rate of thermal diffusion, and thus the least noble element is removed there. This can lead to grain boundaries "opening" and otherwise being attacked and degraded by molten salt. The corrosion seen in molten salt is a mixture of high attack at grain boundaries, and more uniform matrix surface attack. This can look different based on the specifics of the system, however there is generally a bulk material far away from the salt-metal interface with a zone in between that is depleted in least noble metal that has porosity and attacked grain boundaries. Good examples of typical corrosion behavior in molten salt are seen in Figure 2-2.

Corrosion often occurs in other systems such as in LWRs, however it is not a significant concern the way it is in molten salt for a simple reason. In aqueous systems corrosion is thermodynamically favored but is highly controlled by the formation of stable oxide films on the surface of a material. Cr, Al, and a few other elements are often added to alloys and when oxidized they form a layer of metal oxide on the exposed surface of a metal. This surface oxide prevents any further oxidizing agent from reaching metal, and thus prevents corrosion. Molten salt cannot use this scheme to prevent corrosion, as metal oxides are soluble in halide salts. The inability to form stable thin films means that the focus of corrosion control in molten salt must be placed on the chemistry of the salt, the thermodynamics of the alloy, and how they interact to produce beneficial or problematic behavior.

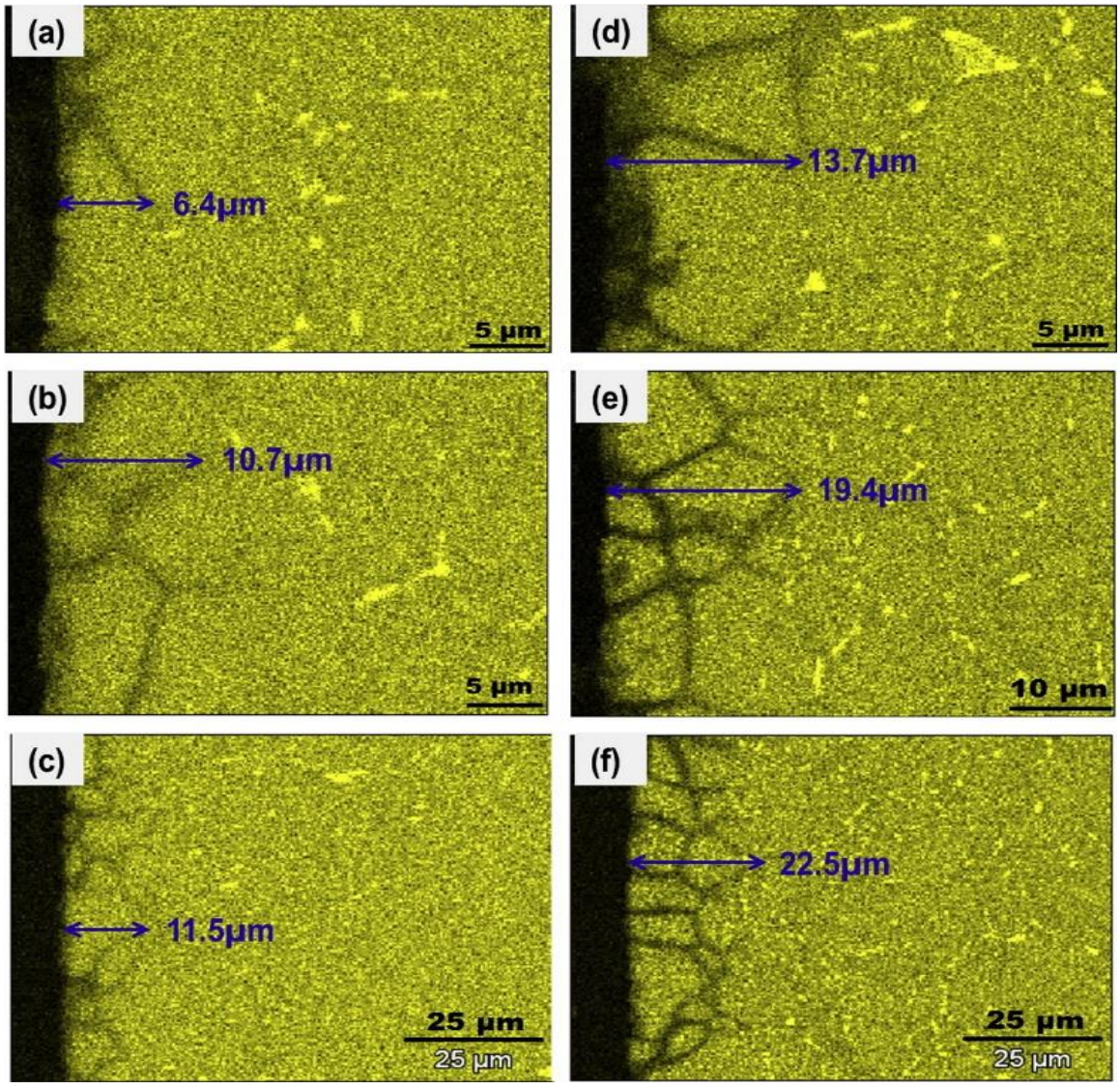

Figure 2-2: Cr Depletion EDS Images

EDS maps of Cr distribution in 316 steel exposed to FLiBe Salt at 700° C. (a)-(c) were in 316 capsules, (d)-(f) were in graphite. Exposure times were 1000 hours for (a) and (d) , 2000 hours for (b) and (e), and 3000 hours for (c) and (f). This figure shows surface depletion of Cr, the least noble metal, and depletion along grain boundaries. [25]

Impurity importance

The importance of impurities on material corrosion by molten salts cannot be over-stated. Literature work has shown that when considered against other factors, the purity of salt provides much of the determination on how corrosion occurs[25]. Multiple types of impurities occur in molten salt. Metals not intended as a part of the salt may be included. A common example of this is iron content in salts due to contact with stainless steel working tools. There may be oxide in salt from any contact with oxygen. Oxide content is highly important in determining molten salt corrosion behavior, as it allows some salts the ability to form oxides from the metal originally in the salt and free halide anions to react more metal. An example of this would be in a NaCl-$MgCl_2$ salt at the eutectic mixture of 32-68. If exposed to dry air this salt would form MgO and Cl_2. The presence of free Cl would lead to increased corrosion. More common than this is the contaminant H_2O. Water is a highly problematic contaminant in molten salt, as in the example previously discussed, the $MgCl_2$ would react with H_2O giving MgO and 2 HCl. HCl is highly corrosive to metals and would lead to degradation of materials at a faster rate. Both papers by Ouyang studied corrosion in a FLiNaK salt that had high moisture content, and thus high corrosion rates [26, 27]. The problem with water is of particular significance since the salts being considered for molten salt systems are highly hygroscopic at room temperature, with $MgCl_2$ naturally forming $MgCl_2 * 6H_2O$. This problem means that much of the published data in molten salt corrosion studies is not particularly useful, as without characterization of the specific impurities of the salt there is not a retroactive way to understand the role that impurities may have played in the corrosion results.

The potential solutions for dealing with the purity problem for molten salt are varied. Some groups use chemical cleaning processes to remove excess oxide. Other groups use vacuum distillation to purify salts. There is not a clear comparison of these two methods or any other purification methods in literature. There is also not a metric used to compare

the purity of salts used in literature, which might provide clarity on some experimental results of the past.

The solution proposed in the MSRE was to limit chemical corrosion and deal with impurities using salt chemistry. Salts were prepared with minimal contaminants, and any H2O or O impurities became unimportant once chemical control of the salt was obtained, as produced F was reacted with Be metal additions. The proper chemistry of the salt was maintained by monitoring the amount of UF_3 to UF_4 such that a known state was maintained. This limited corrosion and chemical issues for the MSRE, however a better system of monitoring this ratio is needed for a new MSR. When the UF_3 to UF_4 ratio was found to be deviate from the desired ratio, the addition of Be metal to the salt (FLiBe) was used to shift to having more UF_3. Similarly, a greater pressure of HF could be maintained to increase the amount of UF_4 if the salt was found to be too reducing.

General trends between chlorides and fluorides

Halide salts generally have been discussed this far, and no significant distinction has been made between the chlorides and fluorides. The two have many similarities thermodynamically. Elements that are more noble in one tend to be noble in the other with few exceptions. Both tend to from compounds in similar ways, taking the form of a singly charged anion when bonding to a metal. Fluorine is generally thought of as the less corrosive of the two, breaking trend with much of chemistry where fluorine is highly reactive. The reasoning for this is the high reactivity that would imply fluorine being more reactive leads to it not forming some of the more complex reactions that chlorine can. Chlorine in the presence of oxygen and the right redox conditions may form hypochlorite anions that provide alternate ways to oxidize metal. Chlorine is able to form other species, particularly with impurities that lead to more possible reactions with the metal in question. This increases the ability of Cl based salts to corrode metals in molten salts.

In addition to the problem of Cl generally being more difficult chemically, there is simply less data for the chloride salts than for the fluoride salts. Fluorine was chosen for some very good reasons for the ARE and MSRE, and much of the testing data for those programs has informed further work. The data that does exist for the Cl salts tends to be from papers on the topics of electrochemistry, Pyroprocessing, and solar thermal energy storage. All of these applications have slightly different requirements than what is needed for nuclear applications based on the challenges of dealing with neutrons.

A final challenge for molten chloride salts is that of neutronic properties. Fluorine has one isotope, and a relatively low neutron absorption cross section. The importance of this for a molten salt reactor cannot be understated. A chlorine salt could only be used to breed fuel with a fast neutron spectrum. Additionally, unenriched Cl salts would produce Cl-36, an undesirable radioactive activation product with a long half life and high energy beta emission [28]. For these reasons, the implementation of a Cl salt has technical challenges that fluorine salts do not experience.

The Cl salts have some advantages worth discussing from a physical properties perspective. They have higher heat capacities, higher densities and lower viscosities than fluoride salts. Cl salts have a clear advantage in physical properties, however either salt could potentially be used successfully to operate a reactor. The choice of balancing chemical, nuclear, and physical properties is not clear cut, and depending on the specific requirements of a project or program, both chloride and fluoride salts are viable options for a MSR and that neither chloride or fluoride salts are a clear choice.

Redox state control

Corrosion behavior often shows radically different results if proper controls are taken to limit the corrosive nature of the salt. There must be tight control of the redox potential of a salt for a MSR, as a salt with too many additions will not hold fission products and fissile material in solution and instead leave high contamination at various places in the system. On the other hand, if a salt is too oxidizing, metal from the containing system

will be oxidized and no longer contain the salt. The solution is to use proper redox state control to ensure that these problems do not occur. Redox control is maintained by three control mechanisms. First, metallic additions are used to reduce the halide potential and make the salt more reducing in nature. These additions are usually made in the most noble metal that is used in the salt, e.g. Be in a FLiBe salt. Studies of corrosion involving least noble metal addition have shown reduced attack [29].

The second control of the redox state of a molten salt system is that of a halide gas overpressure. By maintaining a small volume of halide gas that may react with a more reducing salt, proper chemistry can be maintained. This is a much finer control than metallic additions, only slightly shifting the redox state of the system. The presence of free halide gas means that there will be exchange with the salt, and if it becomes more reduced, the greater availability of metal to oxidize will lead to reaction with the halide gas overpressure. This will help prevent large shifts in redox state.

The final tool for redox control is the use of a multiple oxidation state cation. U, Th, Ce, Zr and a few others are proposed for this purpose. These metals may take multiple oxidation states based on how oxidizing or reductive the salt is. The purpose of using a redox couple is to prevent rapid shifts in the state of the salt that may be buffered by these elements changing oxidation state. Should salt chemistry change, more of one oxidation state is produced, keeping material in solution or preventing corrosion but absorbing that chemical change. A second benefit besides buffering change is to act as an indicator of the redox state of the salt. As previously mentioned the MSRE used the U(III)/U(IV) couple to determine the redox state of the salt.

A brief paper by Donald Olander describes the above [30]. This relatively short paper is one of the more important papers in the field of molten salt, as it captures many of the most important features of the complex chemistry of molten salt systems and describes what control of molten salt chemistry looks like. While short, the detailed chemistry and relative impact that this paper describes paints a useful picture for understanding the

chemistry required to keep molten salt systems working. This paper is similar to the above description, considering the relative importance of metallic additions to adjust redox state towards being more reducing, multiple oxidation state cations being used to buffer a system, and the use of halide gas to force the system to be more oxidizing. This brief paper is central to what the operation of a real world MSR would look like.

Corrosion testing

A significant amount of data exists on the corrosion of alloys in molten salt. Stephen Raiman recently performed a literature review and data analysis of the available data [25]. A summary of his analysis is presented in Figure 2-3, which captures the relative importance of several factors in the severity of corrosion seen in molten salt systems. The importance of purifying salt is generally more important than the type of salt, the type of metal exposed, or any other factor studied in that work. Another important conclusion from this paper is that data needs to be scrutinized and improved handling procedures need to be adopted by research groups. Two different groups may use the same salt but have different handling or procedures that results in different outcomes.

Much of the data that exists on the corrosion of molten salt systems exists from static corrosion tests where salt is put in a graphite crucible or another inert container material and a sample coupon is exposed. After a specific time, the alloy is removed and the sample is weighed to record the amount of mass change that has occurred in the specimen. Exposed samples are then characterized under electron microscopes to show the microstructure that has developed at the salt-material interface. A good example of this type of study is the paper *Metallurgical study on corrosion of austenitic steels in molten salt LiF–BeF_2* [31]. The advantage of this type of study is that it acts as a good screening test to tell if an alloy will have catastrophic failure in molten salt. The majority of works detailing the corrosion in molten salt are detailed and considered in the literature review by Stephen Raiman [25].

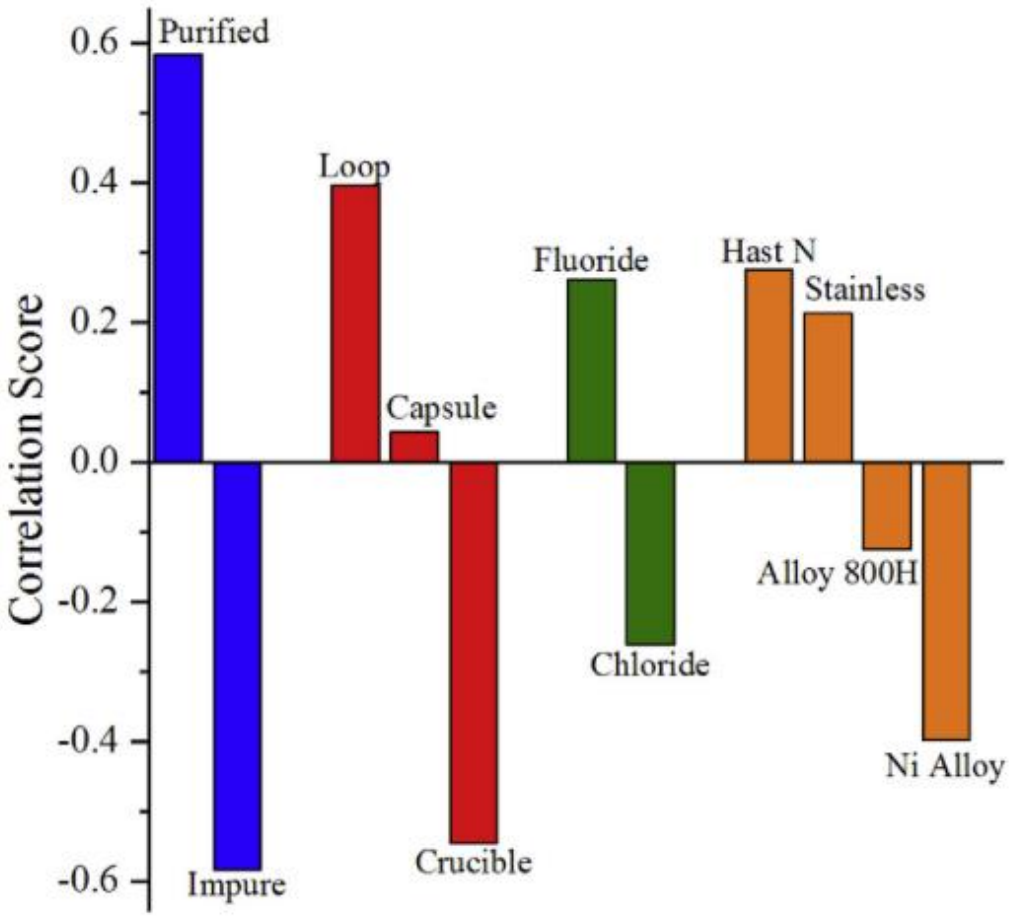

Figure 2-3: Relative Importance of Molten Salt Corrosion Factors

This chart shows the correlation between several factors that influence corrosion in molten salt and their relative importance. It is important to notice that the purification of salt is more important than the alloy exposed. [25]

Continuing corrosion work has studied many facets of molten salt corrosion outside of the more basic factors. Pure Ni coatings are one proposed solution to the problems of corrosion and loss of Cr from alloys immersed in molten salt. Ni coating appeared to slow the loss of Cr, but Cr was lost as it eventually diffused through the Ni coating[32]. There were some other possible positive trends seen, and coatings may be a solution to the problem of corrosion in molten salt.

Another useful and interesting paper discusses Ni-containing salts for pyroprocessing of spent nuclear fuel. Corrosion was found to be low for most situations, however it was found that when excess Li metal was present, Ni was reacted and found is the salt by ICP-OES[33]. This result helps to show that corrosion testing is essential, as predictive work for molten salt is limited.

Loop tests were conducted at ORNL in preparation for the MSRE operation and following the MSRE shutdown. These loops provide data that are highly important, as loops capture many physical features that static tests do not. The flow through a loop is important, however the most important feature seen in loops is that of a thermal gradient. Thermal gradients shift the equilibrium of chemical reactions occurring, resulting in mass transference from the hot to the cold leg of the loop. The work [34] discusses the results from one natural circulation loop at ORNL. Reference [22] further discusses the work, and reaches the important conclusions that metallic additions can help reduce corrosion in salt, high impurities can increase corrosion rates, and voltammetry can measure impurity concentrations. This work also found that there was an initially high corrosion rate as impurities reacted with the structural material. It was found that these impurity reactions eventually react to completion and the corrosion slowed. Be additions to the salt were found to further improve the corrosion resistance of the metal.

In one ORNL technical report, a Hastelloy N thermal convection loop was run for over 9 years [35]. The molten salt was FLiBe (as used in the MSRE), the maximum temperature was 760 C, and the minimum temperature was 593 C. Mass transfer occurred from the

hot to the cold leg of the loop, and the loss of material was found to be moderate, with ~4 mm maximum depth of attack in the hot leg of the loop. Losing 4 mm of material after 9 years is likely a rate that can be managed in reactor designs, however the deposition of this material is likely problematic in the cold leg. The report states that this is significantly improved performance over steel, which is important in the modern discussions between which material should be used in molten salt. It is worth noting that a leak led to the end of this experiment. While this work did show that the bulk alloy can withstand salt for extended times, limitations may be found at joints and welds.

Work has been conducted in Russia in alloys that duplicate Hastelloy N [36]. The corrosion features and results found match well with historic work from ORNL and provide good validation for the ideas presented. This is an important set of work for several reasons, most especially, it is validation from outside of ORNL that Hastelloy N exposed to molten salt is a good combination.

Thermal convection loops importance and chemistry

Gathering the data that informs the thermodynamics and physical processes requires running experiments. The experiments used have advantages and limitations in the data they produce that are worth considering. It is important to discuss the information different kinds of tests can and cannot provide with regards to molten salt corrosion. Static tests such as capsules and crucibles produce results that are the result of being at a specific thermodynamic equilibrium and moving toward it. Static tests act as a sort of screening test in which corrosion is expected to be detected wherein if corrosion is large during static testing, it is expected to be even larger in loop tests.

Loop tests of molten salt are most important, as they activate the physical processes that capsules do not capture. Loop tests produce the changes in temperature across a molten salt system that result in shifting chemical equilibrium. This differing chemical equilibrium from one part of the system to another leads to mass transport through the system, the key feature that creates continuing corrosion at long time intervals. The

importance of getting loop tests and their data cannot be understated. No reactor design will ever be based on a fully static isothermal system. Salt will be pumped and moved throughout a system to transfer heat and be chemically processed. The changing temperature of molten salt is a large problem, as the equilibrium reactions of the system are highly temperature dependent and will create corrosion that might be a significant problem.

A thermal convection loop is the system that has been used to study flowing molten salt systems. Pumps for molten salt are difficult, costly and have limited availability, thus natural circulation is often used to study flowing salt. Natural circulation occurs when part of the loop is heated, and part is allowed to emit heat. This temperature difference leads to thermal expansion of the salt that drives flow. The high viscosity and low thermal expansion coefficient of molten salt mean that a large temperature change is needed to create appreciable flow in molten salt. The temperature difference is often around 100 C, and only results in flow rates of several cm/s. This slow movement gives much time for chemical reactions to occur. The reactions that have been discussed previously all have an equilibrium final state that they are moving toward. In a flowing system, the reactions do not saturate in the same way. As previously discussed, the thermodynamics of the reactions of molten salt with metal are controlled by temperature, taking the form: $M + X\,Ha \leftrightarrow MHa_x$. This is an equilibrium reaction, and differing conditions can shift the balance of this reaction, leading to more or less metal being the preferred thermodynamic state. Generally increasing the temperature of a molten salt will drive the reaction to the product side as written. This means that more metal can be reacted and subsequently dissolved in a high temperature salt compared to a low temperature one. Similarly, in a low temperature salt, less metal can be oxidized as MHa_x, and metal must be formed. This temperature has little bearing on static tests. However, for a thermal convection loop this means that metal is reacted and removed as the salt is being heated. Higher temperatures favor the production of the metal halides in the system. Similarly, as the salt is cooled, metal is removed from the salt and deposited

out of the salt, as there is an excess of metal halide in the salt. This process leads to mass transfer from the hot leg (heated section) to the cold leg of the thermal convection loop. This is highly problematic, as it means that corrosion does not naturally slow or stop over time in these systems. The changing temperature and shifting thermodynamic equilibrium of the convection loop means that it will continue to corrode long after a static test will have reached equilibrium. This also means that material will continue to deposit on the cold leg so long as the loop operates. This is a potentially severe problem for any system intending to use molten salt to transfer heat, as it means that metal will be deposited in a heat exchanger as the salt is cooled there (possibly leading to plugging of flow channels in the heat exchanger).

Results from molten salt corrosion loops generally show continuing mass transfer over time, with slowing rate. In some cases, the mass loss is proportional to the square root of the time elapsed [18]. For these experiments, the accepted rate limiting step preventing faster reaction and mass transfer is diffusion of least noble metals through an alloy. Surface depletion of the least noble metal means that diffusion must occur for more corrosion to happen. This slows the rate at which metal is oxidized and mass is transferred. This sort of understanding of how corrosion will proceed is needed for future MSR designs and shows why thermal convection loops are an important tool to understand how reactor systems will behave.

It is worth mentioning in this section that a few pumped corrosion loops were run at ORNL. These systems used pumps to move salt resulting in flow rates that were much greater and more relevant to MSR systems. The loop MSR-FCL-2 was designed with Hastelloy N and the salt for the MSBR project. Limited studies of the corrosion in this loop exist, but the corrosion rate was minimal for this loop, showing that there was not a significant impact by flow for molten salt flowing in the low m/s range[18]. Further molten salt forced convection loops were planned to further study the effects of flow on molten salt systems. However with the end of the MSBR program these loops were never built. The designs for two loops are documented in a report [37].

LIBS Technique

Introduction

LIBS is an advanced characterization technique that studies the elemental composition of a sample. LIBS fires a laser at the sample creating a plasma the emits light which is analyzed. This is repeated until the selected process has been run. The emissions are then analyzed to provide results of what elements are present. LIBS has benefits and limitations compared to other techniques that will be discussed later in this work.

Process of LIBS data Collection

LIBS begins with pulsing a laser at high power onto a sample. The high energy density created by a focused high-power laser on a surface produces intense localized heating and creates a plasma from the material corresponding to the area the laser was focused on. This plasma cools when the laser pulse is turned off, and during its cooling emits coherent light characteristic to the elements present. This atomic emission spectra can then be used to determine what elements were present and calculate the fractions of each. Quantitative LIBS requires calibrating the system with known references so that the specifics of the spectrometer used are well understood. It is also important to know the power used in the laser producing each plasma, as slight variations in plasma temperature can lead to different optical emissions from a plasma. LIBS can be conducted under an inert atmosphere instead of in a vacuum, since the production of plasma of the cover gas can usually be separated from that of the sample. In our specific work, Ar was used as a cover gas. This led to difficulties in being able to see Cl, since their emissions overlap in the region of visible light that we collected in our spectra. This issue would not occur if a different cover gas were used in place of Ar, He is an ideal choice as it has very few emissions, however Ne would be a more cost effective choice.

A final and important consideration when discussing LIBS is that of its ability to be done in situ on samples that cannot be moved, or portions removed to characterize. LIBS can be done remotely through a clear window, or through a fiber optic cable.

LIBS data analysis

For simple analysis of what is present, LIBS spectra can be studied and compared to standard atomic emissions [38]. The default way of doing this is to use the software included with the LIBS instrument to develop an analysis that integrates the emission lines seen from specific elements. Simple numeric integration over the set of wavelengths that capture the emission peak of the cooling plasma with the background black body radiation removed is a common way to measure the amount of an element present in a sample. This method is simple but has problems with elements that have overlapping emissions, and/or overly intense emission lines. If the intensity of an emission is sufficiently high, it can exceed the maximum allowable intensity value in a detector, making it impossible to know its actual intensity. For these reasons, it is important to carefully consider what emission lines are used for analysis. This high degree of input must be considered carefully to ensure that it accurately reflects the sample studied. Advanced numeric techniques such as Principal Component Analysis (PCA), Non-Negative Matrix Factorization (NNMF), and Multiple Component Analysis (MCA) might be of benefit, as they will not require the manual input of emission peaks to find signals, and they might enable the separation of more complex trends that cannot be seen with univariate analysis.

Benefits and Limitations of LIBS relative to EDS, GDOES, etc.

LIBS has several benefits over other characterization techniques. Chief among the benefits LIBS offers is that of being very rapid to conduct with minimal sample preparation. Samples can be studied without special preparation. For example, salt can be left on the surface of a sample and LIBS could be conducted. In this case, the LIBS

instrument would “burn” through the surface layer of salt and study the interface and metal underneath. Other characterization techniques most often need sample preparation where a sample is mounted in epoxy, is cut in half, polished or otherwise prepared. LIBS does not require this, making the sample preparation much easier than that need for other analysis techniques.

LIBS has benefits compared to EDS in what elements can be imaged. EDS relies on the production of X-rays, light elements produce low energy x-rays that are not able to be detected well due to absorption in the x-ray detector pathway, and their lack of electrons makes this a less probable event than producing an x-ray in a higher atomic number atom and thus EDS has difficulty imaging low Z elements such as Li. LIBS has no such problem, as these light elements do emit light while cooling as a plasma. This benefit makes LIBS ideal for situations requiring characterization of low Z materials.

Glow Discharge Optical Emission Spectroscopy (GDOES), Inductively Coupled Plasma Optical Emission Spectroscopy (ICPOES), and other optical emission spectroscopy techniques are quite similar to LIBS in what elements they are able to detect. These techniques all work by producing a plasma that cools and emits coherent light which can be studied to determine what elements are present. The advantage that LIBS provides is that LIBS allows for finer spot sizes. Work comparing the two techniques exists and reaches the conclusion that for homogenous samples such as thin films, GDOES shows slight advantage over LIBS. In cases where lateral resolution is important, LIBS more clearly characterizes the material than GDOES [39]. One of the most important considerations justifying LIBS as a useful technique compared to GDOES or ICPOES is that of being conducted in-situ. Samples do not need to be removed and transferred to an instrument. Instead the LIBS instrument may be brought to the material of interest for use.

There are physical processes that occur during LIBS that need to be considered and accounted for to produce the best possible results. To study the plasma created by the

laser pulse in a LIBS system, a delay must be used between when the laser fires and when the spectra is taken. This delay allows the plasma to cool and have less black body thermal radiation in the region of the spectrum that is studied. This reduces the noise in the spectra measured with LIBS, and results in more useful analysis. The problem with this is that cool plasmas do not activate some emission lines. Some characteristic elemental emissions are not present if a plasma is not sufficiently hot. For these reasons, adjusting the delay of the spectra gathered in a LIBS instrument can make a large difference in the analysis. Default gate delays are usually around a few microseconds for most materials. These can be calibrated, however gate delays over a microsecond are usually sufficient to eliminate black-body radiation of cooling plasma. A second important physical process occurring in LIBS is that of ablating into a material. When a plasma is created, it removes a small layer of material on a sample's surface. When the next laser pulse occurs hitting the sample, it is not as well focused, and does not deposit energy as well. This effect is small, but may be important for complex analysis of LIBS data and for depth-dependent analysis. In addition to looking at a region of material further into a material, another process occurs after a laser pulse in LIBS characterization. The cooling plasma from a laser pulse is often deposited on to the sample surface near where it was created. This re-deposition of material generally needs to be considered as it could lead to false conclusions if not accounted for. For example: If a pure Ni sample was coated with Cu and LIBS was used for depth-dependent characterization, Cu would likely be detected to some depth in the material due to the re-deposition of material from the previous plasma. In addition to re-deposition of material, as LIBS reaches deeper into a sample, there is a loss of geometric efficiency to the detector, meaning that the signal deeper in to a material is artificially reduced in a way that does not capture the reality of the situation. For this reason, it is useful to normalize elemental emissions to an element that should be invariant as a function of depth.

Additional concerns with LIBS are associated with the specific way that elements' emissions overlap. For example, in standard optical wavelengths, it is almost impossible

to quantify Cl concentrations if Ar is used as a cover gas for a sample. This occurs because the many strong emission lines from Ar happen to overlap the few emission lines from Cl that fall in the visual range. There are techniques that could allow for the specific characterization in this case: Laser Induced Fluorescence, and molecular emission studies in addition to LIBS. However substituting a different noble gas as a cover gas would also be a solution to this specific interaction[38]. The interaction of Cl and Ar emissions is mentioned due to its relevance to this thesis work, but other combinations of elements can similarly have overlapping atomic emission spectra that create problems for analysis.

Previous LIBS work

There is not significant prior work in the literature using LIBS to characterize molten salt corrosion and salt-sample interaction. There is some published work on using LIBS to characterize aerosolized molten salt to determine the uranium content [40], however this is significantly different from the LIBS characterization in the context of the current thesis work. Similarly, there is work demonstrating the measurement of Eu and Pr in molten salt [41], but the same caveat as before applies about the work being significantly different. The limited amount of work that uses LIBS to study molten salt is focused on characterizing fission products, rather than characterizing corrosion.

In literature, work has been done on sets of spectra collected from LIBS that required more complex analysis [42]. In the literature case, they used LIBS to study multiple phases of rocks in a geologic specimen. Principal Component Analysis was applied to the acquired LIBS data in order to determine what portions of the emission spectra changed as a function of location and depth ablated into the material. For this case, it meant that the authors were able to create a heat map of the differing phases of the rock present, which matched with their optical imaging of the same. This work demonstrates that more sophisticated computational analysis of LIBS data may enable more refined analysis and provide further insight.

CHAPTER THREE METHODS

Description of molten salt corrosion experiments

The experiment that was used to produce the molten salt exposed samples was conducted as a part of an LDRD project (S. Raiman, PI) conducted at ORNL. A matrix of Ni-based samples with differing Cr content were exposed to molten salt for a selected amount of time sufficient to induce measurable corrosion. Samples exposed were binary Ni-Cr alloys with Cr contents of 7, 16, 24 and 100 atomic percent. Samples were exposed for 100, 500, 1000, 2000, and 2500 hours. Samples were exposed at 700° C and 800° C. This is detailed in figure 3-1. A high degree of control was used when preparing the molten salt for these specimens. The salt was a eutectic KCl-$MgCl_2$ mixture. Salt was characterized and found to be less than 5% H_2O content [43]. The salt was purified using the method outlined in *Purification of Chloride Salts for Concentrated Solar Applications* [44], which should result in a salt free of impurities. After production, the salt was stored in an inert Ar glove box until needed for experiments. An experiment consisted of a Mo inner capsule being loaded with salt and a specimen, then that Mo capsule was loaded into a stainless steel capsule to protect it from air and rapid corrosion while at temperature. This capsule also acted to catch any molten salt from cracked Mo inner capsules to prevent damage to the furnace or experiment. This procedure is shown in figure 3-2. The Mo is chemically inert in molten salt given the thermodynamics of Mo in salts; however it is brittle and it is possible for Mo to crack. To prevent the leaking of molten salt, a stainless steel outer capsule was used. Capsules were loaded into a furnace, and held at temperature for the specified amount of time. Capsules were then removed from the furnace and allowed to cool. After cooling, capsules were cut open, samples were “chipped out” of salt, then were washed to remove any remaining salt on the sample surface. After washing, the samples were weighed to quantify mass loss and then samples were cut in half with half retained and half mounted in epoxy to allow for the study of the cross section looking inwards from the salt-exposed surface.

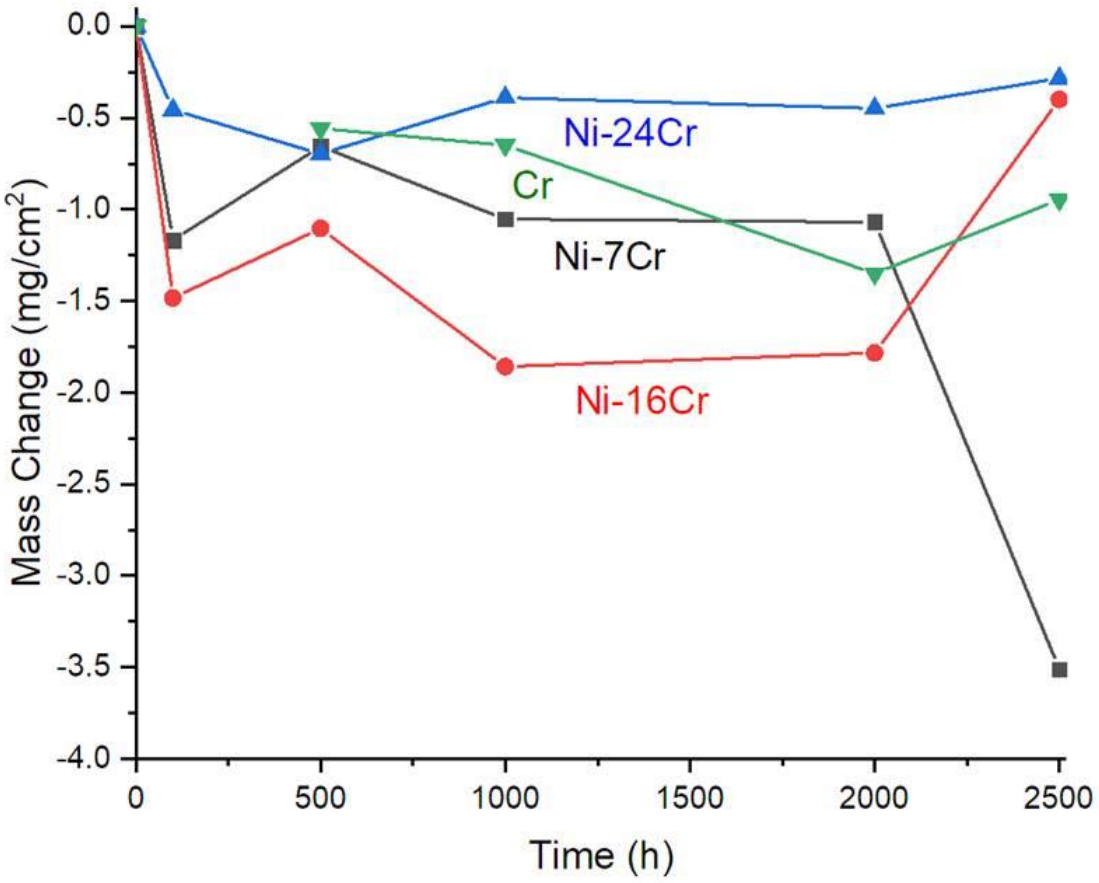

Figure 3-1: Mass Loss Data from Raiman LDRD

Here we can see results of the mass loss measurements from the samples used in this work. The 16% Cr samples were used in this work, thus focus on the red line and data points. [Raiman, unpublished]

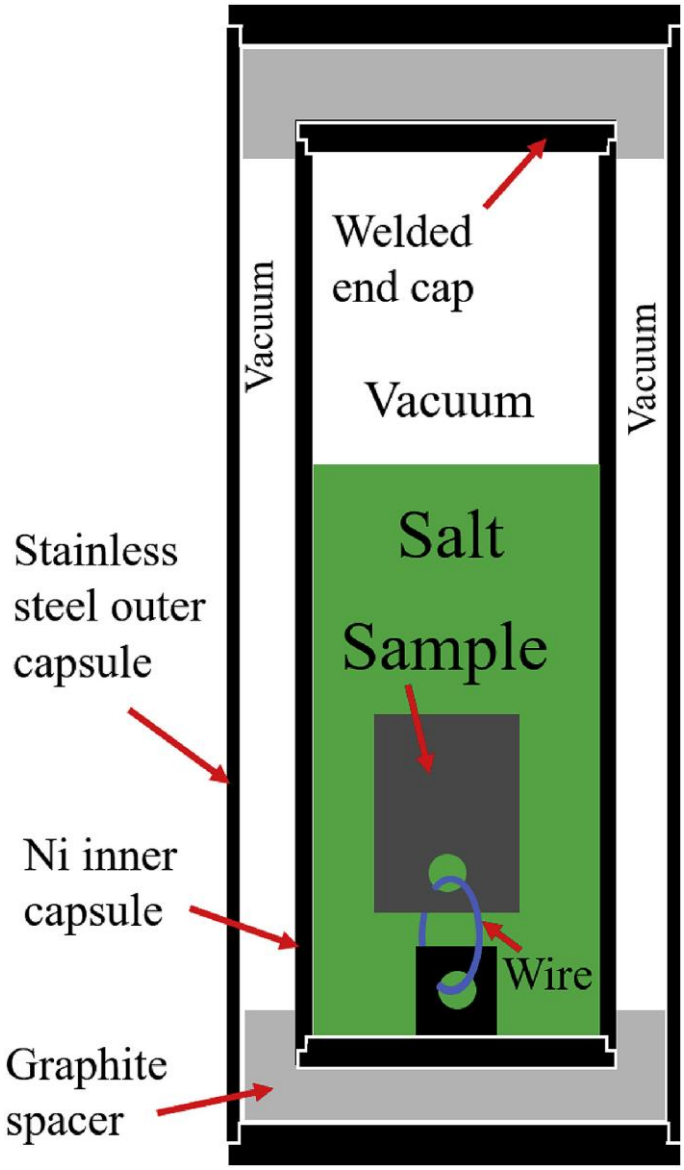

Figure 3-2: Schematic of a capsule containing a sample and salt.

In this figure we can see the schematics of the sample and how it was exposed to molten salt[45].

Description of LIBS analysis

LIBS was conducted on the Applied Spectroscopy J200 Laser-Induced Breakdown Spectroscopy (LIBS) instrument. The retained half of molten salt exposed samples were used for the LIBS characterization. LIBS was run with a 140 μm spot size in a 10 by 10 grid with a total exposure of 200 shots in each location. Laser power was 14.8±.3 mJ per shot. Imaging was done under an Ar inert atmosphere.

Description of LIBS data processing

Initial analysis of the data set collected for this work relied on the software included with the LIBS instrument. The most important (highest intensity and most distinguishable) emission peaks were selected for the elements that were expected to be present. A simple geometric integration of the spectrum in the region of these peaks given the broadening seen was used to give the signal count for each element. This approach met with some difficulty in producing quantitative results, and thus a new approach was developed.

Data analysis using the provided software was not convenient, as it was limited to simple integration and background removal on a nearby region of the emission spectra. A Python code was developed to conduct the analysis and allow for more complex consideration of the data, such as removing regions where re-deposition occurred, and taking an interpolated measurement of the background, both of which should improve performance of LIBS characterization. This code reads in the data, then looks for selected regions of interest. These regions of interest are chosen based on the NIST LIBS database, which shows what emission lines should be strongly seen. From this, the channel number of the wavelength is selected, plotted and the bounds of the emission peak are found. These are input to the Python code, which uses these as bounds to integrate the peak, and subtract the background of the spectra in the region. This process is repeated for each spectra, providing an intensity of each peak at each location where a LIBS spectra was collected.

These can then be averaged and plotted, or all plotted on a single figure to look for variations.

PCA and NMF were implemented in the python code developed for the analysis of this LIBS data. However thus far, the univariate analysis appears to capture what is occurring.

SEM characterization

Before LIBS was conducted, SEM images of the sample surfaces were taken at ORNL HTML. These were gathered on a GE-S3400 instrument with accelerating voltage of 10kV. SEM cross section images and EDS linescans were gathered on a Phenom XL instrument at the stable isotopes group at ORNL. Accelerating voltage was 15kV.

CHAPTER FOUR – RESULTS

Results From LIBS

LIBS was conducted on a set of samples varying in exposure time. All samples studied were of the same model alloy with 16 atomic percent Cr, 84 percent Ni composition. These samples were exposed to a KCl-$MgCl_2$ eutectic mixture (68% KCl). Exposure times were 1000, 2000, and 2500 hours. An unexposed sample of the same model alloy was studied as reference. The analysis of data obtained from LIBS characterization begins with simple integrations of the emission peaks for selected elements. Raw emission spectra from an exposed sample are shown in figure 4-1. This raw data is noisy, but some important initial observations can be made.

The LIBS data were able to show a few major features that appear in these samples. Simple numeric integrations of common Ni and Cr peaks are shown in figure 4-2. First, all samples that were exposed to salt were depleted in Cr at the sample surface, indicating that Cr solute was preferentially removed due to the exposure to molten salt. We can see that there is variation in the Ni signal, however this is a product of the data collection and is not real. This is confirmed with EDS data (figure 4-3), which shows that there is not significant variation in the Ni content of the samples as a function of depth. Instead, the variation in the Ni signal seen in the LIBS analysis is a feature of the LIBS technique rather than a description of the sample. For easier comparison to the EDS data, an ablation rate was assumed for the LIBS at 0.2 μm per shot. This rate is from unpublished work, and will be adjusted later. This is shown in figure 4-4. Here we can see that the shape of the LIBS data and the EDS data are similar. Further work will be done comparing the two in the next chapter.

The second important result from LIBS was that elements from the salt were present at the surface, and Mg and K had different behaviors. The integration of K and Mg peaks

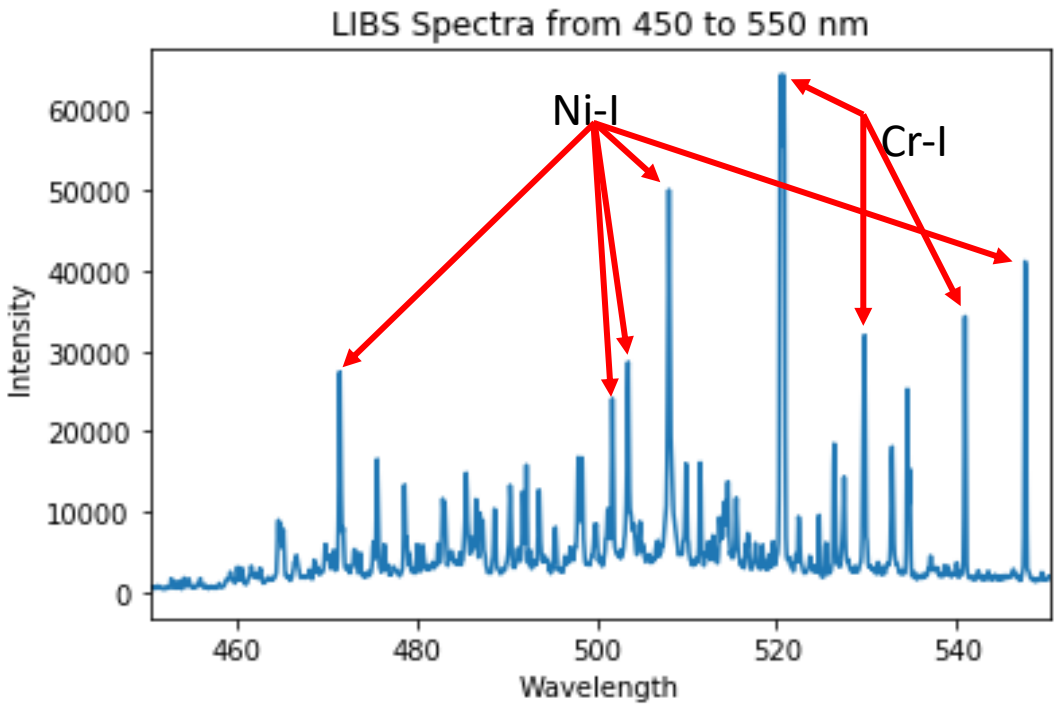

Figure 4-1: Sample LIBS Spectra

LIBS spectra from unexposed sample showing examples of emission peaks and background. Spectra from shot 100 on unexposed sample.

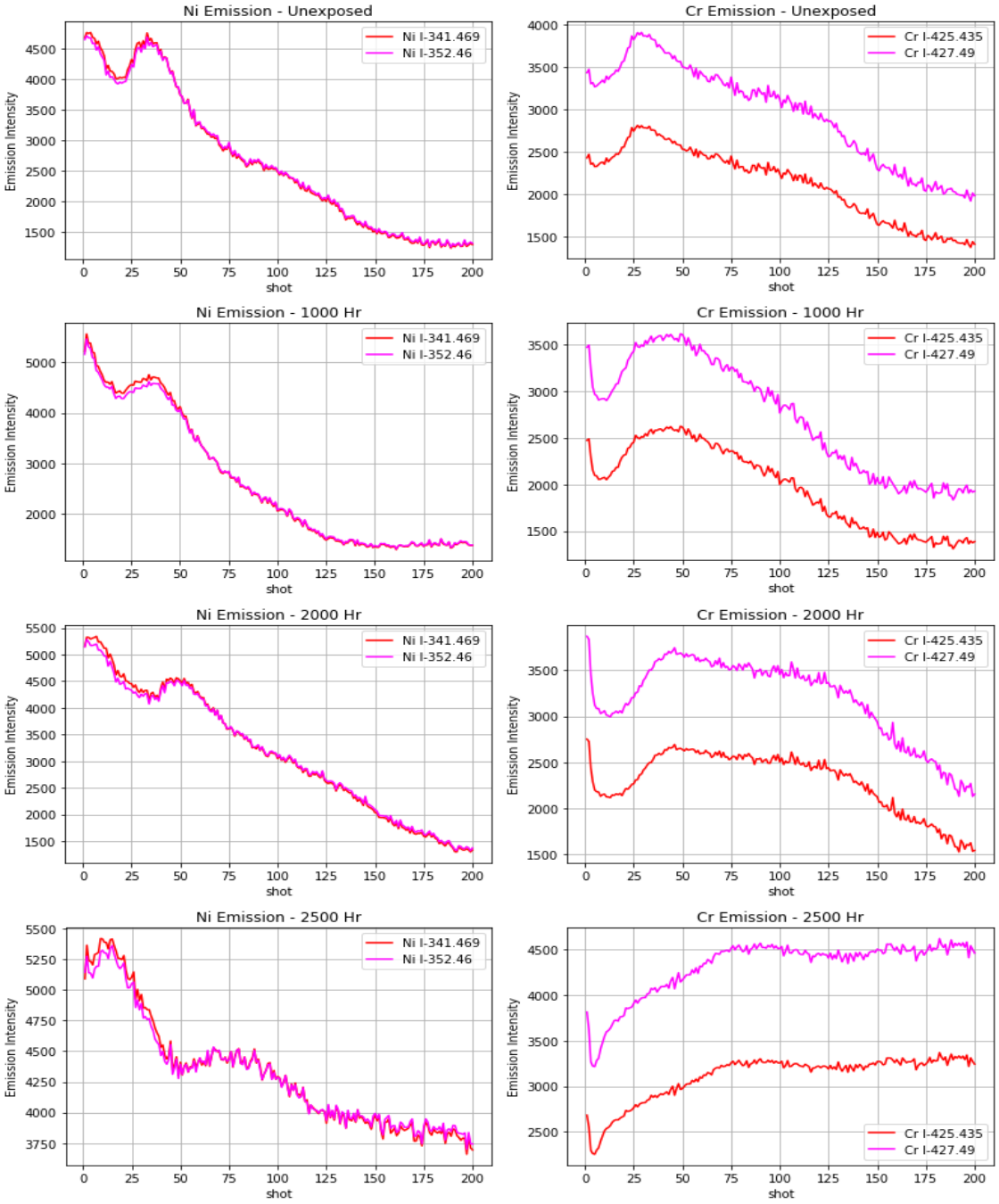

Figure 4-2: Simple Numeric integrations of Ni and Cr emission peaks

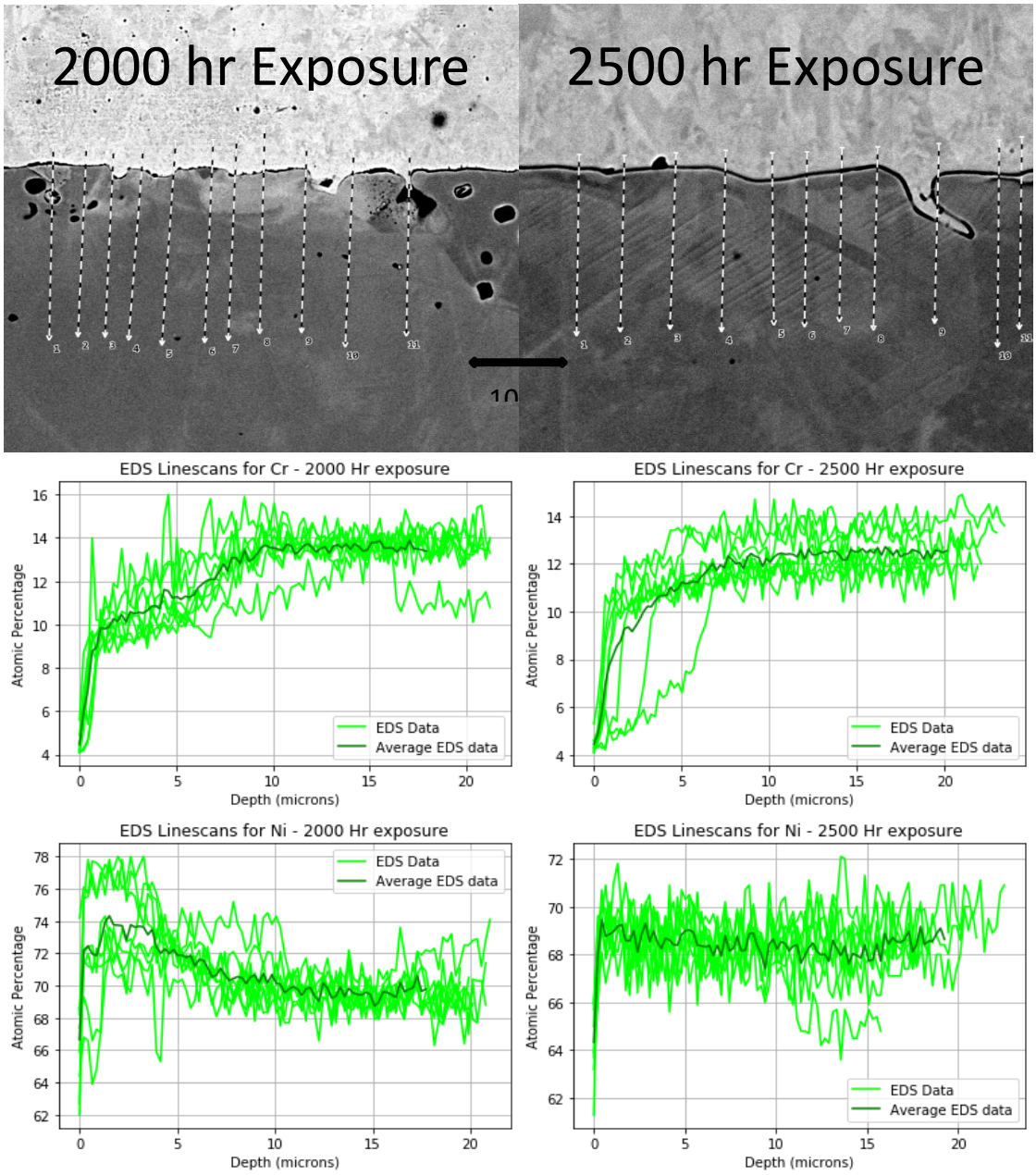

Figure 4-3: EDS Linescans of Ni and Cr and SEM image of interface after exposure

2000 hr and 2500 hr exposure to KCl-MgCl2 salt are shown. Code was used to select region after Cr coating was no longer seen in profile.

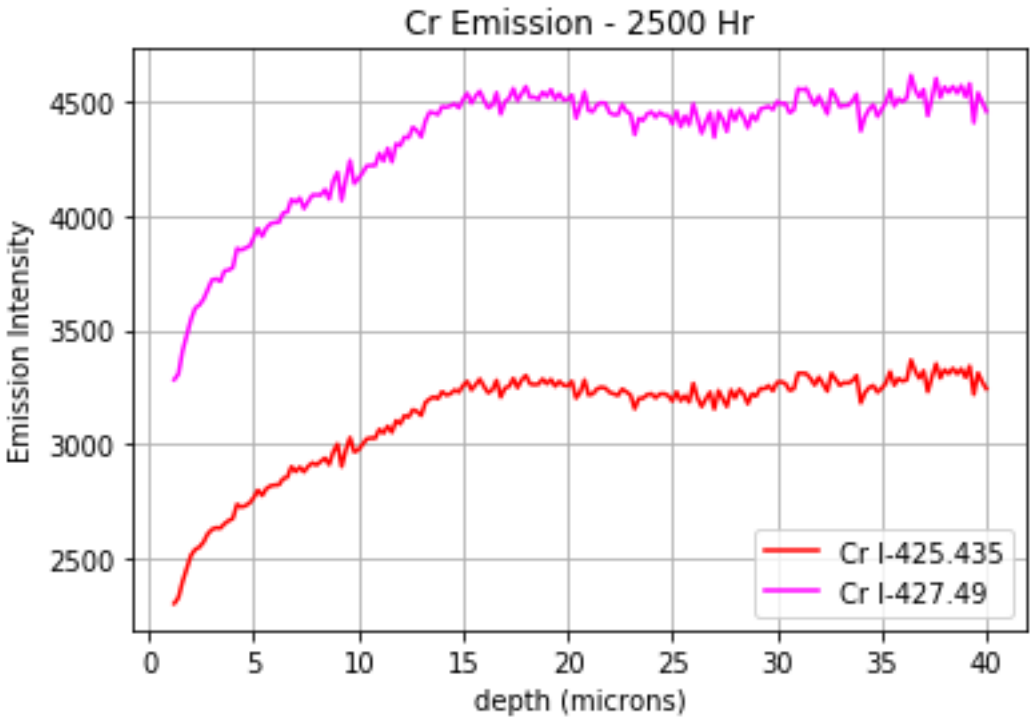

Figure 4-4: Numeric integrations of 2500 hr exposure with assumed ablation rate of 0.2 µm per shot

are shown in figure 4-5. There are several observations that can be made from this figure; first, there were very few locations on the exposed sample surface with entrained K. This means that the near-surface intercalation and trapping of salt is quite rare. A second observation from figure 4-5 is that Mg was found on the surface in most samples. This might be some kind of exchange reaction such as: $MgCl_2 + CrO \rightarrow MgO + CrCl_2$ or this Mg might be present due to the washing process that the samples underwent which exposed them to air and water, both of which could act as sources of O to react $MgCl_2$ to MgO. K was also found to have less intensity on the longer exposed samples, although the detected intensity was always relatively low suggesting that there is limited K even when it is present. The unexposed sample had no amount of K present suggesting that there was not simply a bias in data collection or processing that resulted in seeing this signal.

The detection of Mg created some difficulty in the LIBS analysis. Mg has only one relatively intense emission in LIBS, that being the Mg-II-279 nm line. The second most intense line is a line that sits on the emission peak seen in the 279 nm line, and thus it is not ideal for characterizing the presence of Mg. The third most intense Mg emission is a Mg-I emission around 383 nm. This presents a problem, as these lines will likely not show the same variation with depth, since one is a I and one is an II line. The I peak corresponds to neutral emission, where an electron is moving to a lower energy orbital on a fully filled electron shell. The II peak is a singly charged emission, where an electron is moving to a lower energy orbital in a singly ionized atom. The production of differently ionized species should change rapidly as a function of shot number, since the system will be less efficient at producing plasma as the number of ablations increases, and thus less and cooler plasma will likely result. This complexity makes comparing the results of the Mg-I and Mg-II lines difficult. We can say that there is Mg present to some small extent on all of the samples exposed to salt. Mg appears to be localized to the surface for these cases, and there appears to be limited change in the signal intensity as a function of exposure time.

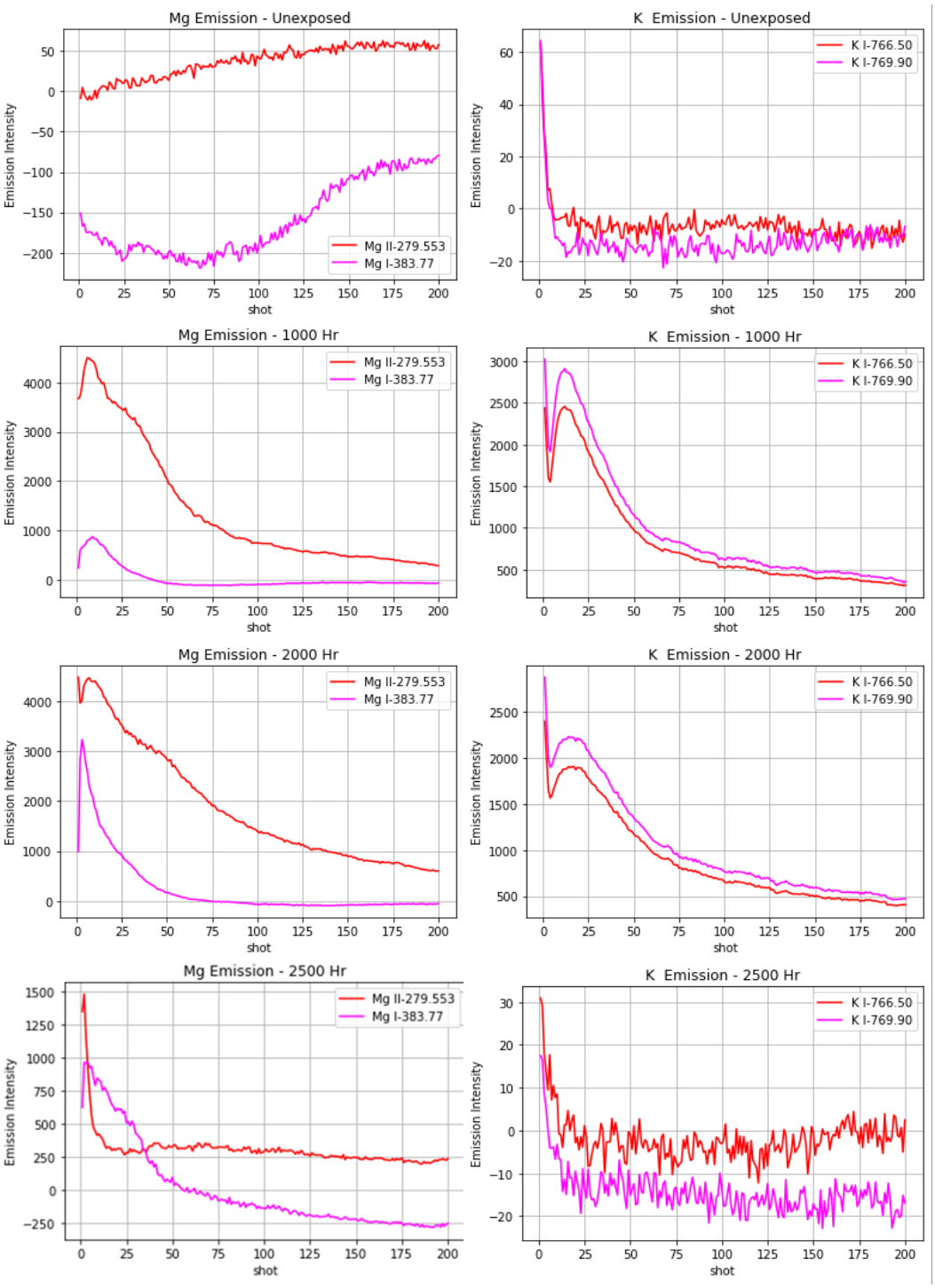

Figure 4-5: Integration of the Mg and K emission peaks for all samples

All of the reporting thus far deals with simple integration of the peaks, which does not provide particularly accurate plots, since variations in the sample characteristics and laser characteristics occurred that create noise. For example in figure 4-2, we can see that the signal from the Ni emission appears to decrease with increasing shot number. However, these data were obtained on an unexposed sample of material and therefore the solute concentration should be constant with respect to depth from the surface. This effect (as mentioned earlier in this work) is associated with the loss of efficiency in energy deposition by the laser, and loss of efficiency in optical emission of the plasma based on the changing geometry of the system (varying crater dimensions with increasing number of laser pulses). To deal with these factors as well as reduce variations that occur from fluctuating laser power, the ratio of the Cr signal to the Ni signal is reported in figure 4-6. This figure shows a few regions of interest at the surface where there is re-deposition of material. There is a peak around shot 20, the origin of which is unclear. One possibility is that this feature is a product of having the focus of the laser below the sample surface. In that case, the signal seen deeper into the material would be larger, as plasma production would be maximized when the focal location of the laser is reached. This feature is seen in all spectra, including the unexposed case suggesting that it is not a product of exposure to salt, but instead something due to the LIBS process. The next feature of interest is that of a relatively linear increase in signal relative to shot number between shots 60 to 140, and a region where the signal does not show significant variance. Note in this figure that there are still some odd features. First, there appear to be multiple regions of behavior as a function of shot number. At the surface (shots 1-3), the sample appears to have localized enrichment of Cr. This signal is a product of the ablation process depositing material back on to the sample and creating an artificial signal in this region. This signal was not a “real” feature of the data, as it was not produced by the molten salt corrosion, and thus efforts will be made to remove it in later sections of this work. Other elements outside of Cr can also be normalized to Ni to attempt to extract more trends. However this has little impact, since they show strong trends without this processing.

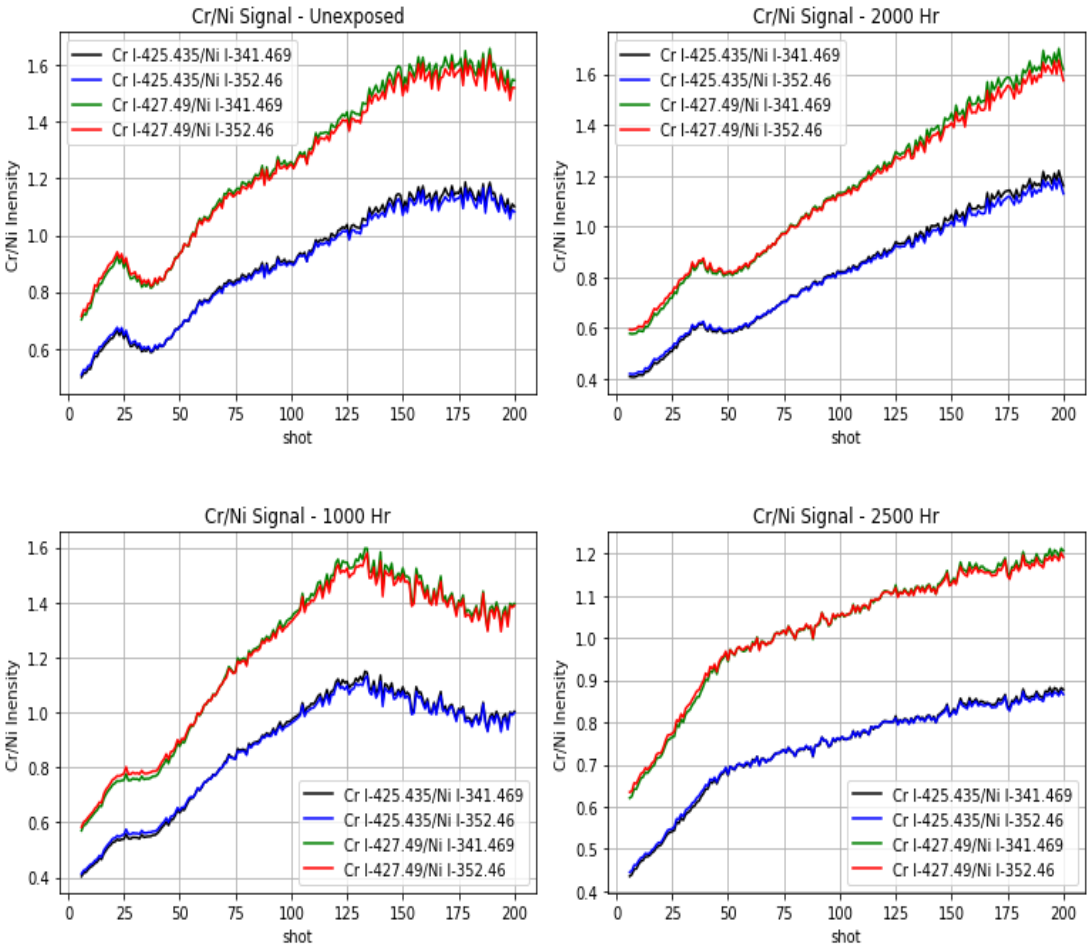

Figure 4-6: Cr signal normalized to Ni signal from same spectra

This correction method should correct for variations in laser power fluctuating between shots.

There is a strengthening of the observed emissions that appear to maximize around shot 24. This feature is not descriptive of the sample, as this feature is not seen in EDS. This feature is likely the result of the focus of the laser being inward of the surface of the material, increasing the efficiency of plasma production as it reaches this depth, resulting in a greater signal. This can be corrected by comparing the signal seen in the exposed sample to that seen at the same peak and shot number in the unexposed sample, as the laser focus was near the same depth. This is done in figure 4-7. Here we can see that the local maximum around shot 24 is gone, and the signal is much smoother. This should also help to account for the changing signal deeper in to the sample, making this a useful correction. Both this, and the previous method will be applied to the same data in the next chapter to attempt to correct for both systematic concerns based on plasma production and based on the fluctuations of laser power that occur in the instrument.

A final small problem that occurs during LIBS is the re-deposition of material at the sample surface. The problem of modified material at the sample surface based on the re-deposition of material from previous ablation is an important consideration in LIBS. In this work, the re-deposition of material can be studied using the surface peak before shot 10 to infer where material has been deposited. To remove this region where material is present from re-deposition, the first 4 shots at each location. By performing this correction method, we know that the region where re-deposition of material occurred was not included in our study. To re-state this process, we remove the first shots of the depth profile until we reach the minimum Cr signal. Figure 4-8 shows the Cr signal with the surface re-deposition feature, as well as the same signal with this feature removed.

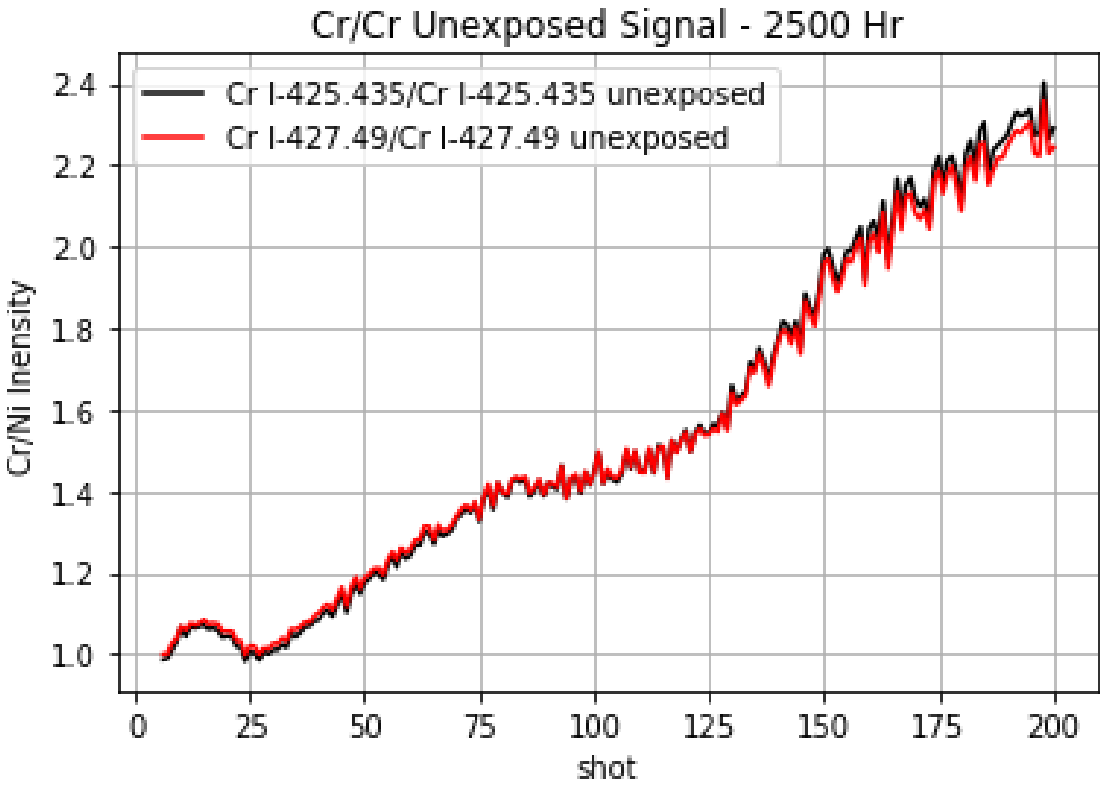

Figure 4-7: Cr signal normalized to Cr signal from unexposed sample to account for variations in sample geometry

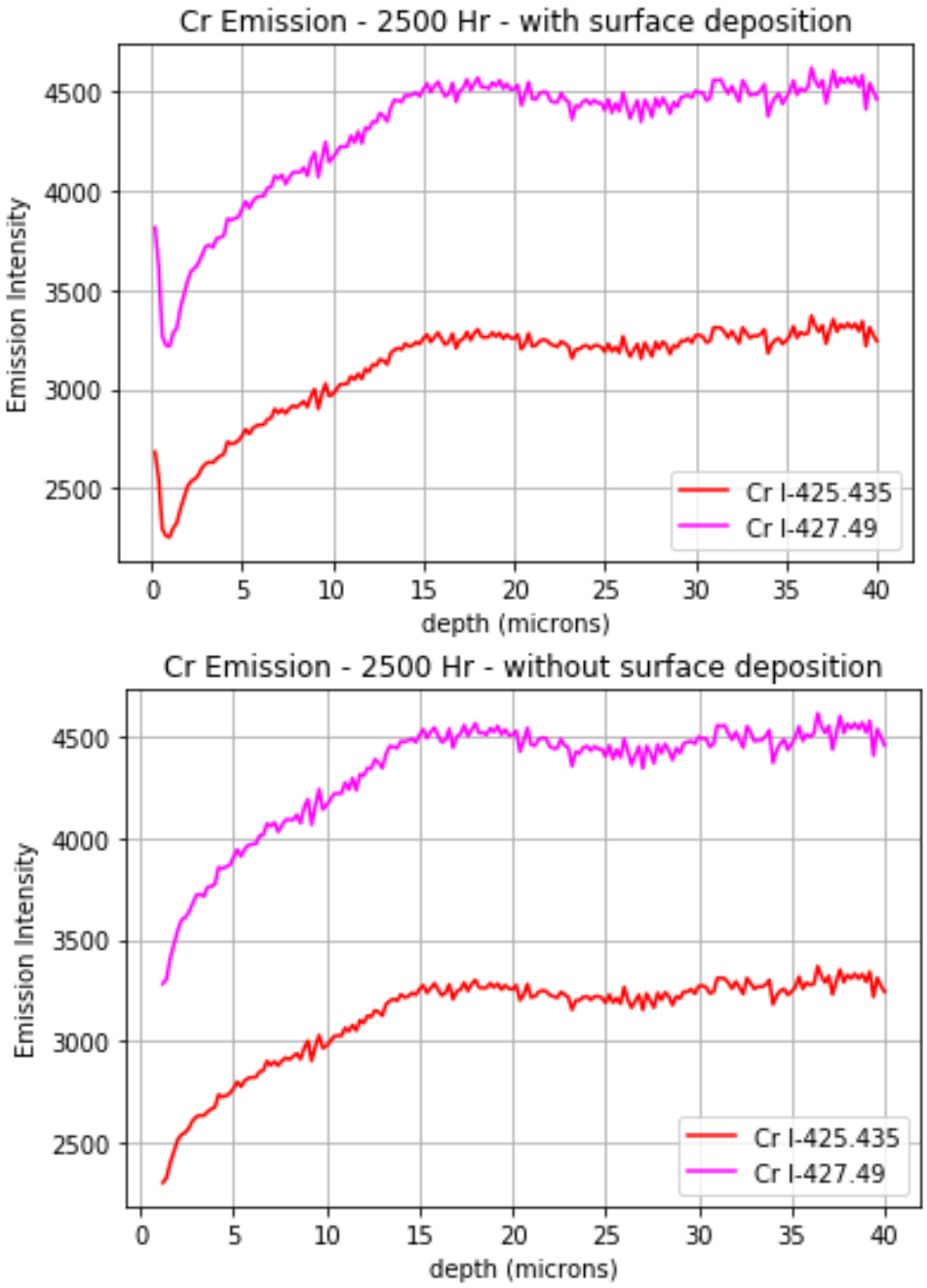

Figure 4-8: Cr signal with and without re-deposition of material at the surface

The 2500 hr sample is shown. Note that the spike seen in shots 1-5 is gone in the lower figure.

CHAPTER FIVE – DISCUSSION

Discussion of results seen in LIBS analysis

There were some consistent trends seen in the LIBS data worth discussing. First, Cr was depleted in the exposed samples near the sample surface. This Cr depletion is unsurprising and matched previous reports in the literature. Ablation rates were not characterized for this work. However literature on similar material at similar power densities results in approximate ablation rates of 0.2 μm per shot. Given that estimate of the ablation rate and a total exposure of 200 shots, a final depth of about 40 microns is reached after 200 LIBS shots. In the exposed samples, the Cr signal appears to reach a maximum and level off around shot 160 after the full set of corrections for geometric efficiency and laser power are applied to the data (figure 4-6). This should map to the EDS data in a similar region, where the Cr content is not significantly changing as a function of depth. The presence of Mg on all salt-exposed samples, and K on some of the samples is strange (shown in Figure 4-5) and merits consideration. It is possible that there is some trapping occurring in some of the rough surface features formed during exposure to salt. Initial thoughts would suggest that longer exposure would increase salt-trapping if this were the case. However it is possible less salt would be trapped at longer exposures, since pores, cracks, and other surface features might become larger and salt might be more able to escape easier from larger surface features resulting in less salt being seen with LIBS. If this is the case, washing would likely remove much of the salt that would be of interest to study. Washing much of the salt away might also explain why Mg is present while K is not. Washing would expose salt to water, which can break $MgCl_2$ to MgO and 2HCl. The MgO would not be soluble in water used to clean salt from the sample, and would likely deposit on the sample. This might explain the presence of Mg on the exposed samples, why K was present in some cases and why their presence differed as a function of exposure time. It is not unexpected then that this is observed, but having Mg and K behave differently is unexpected. The trapping of salt would result in

both K and Mg being present on samples in similar ways. This is not the case, and Mg can be found separate from K in the 2500 hr exposure, where Mg is seen, but K is not (figure 4-5). This trend suggests Mg is present in all samples, while longer exposure times resulted in less presence of K on sample surfaces. One possible explanation is if the washing of samples preferentially removed K in the form of KCl. $MgCl_2$ could also be removed, however $MgCl_2$ in the presence of water will form MgO and HCl. This MgO is not water soluble and might be left behind, leading to different amounts being present compared to the amount of KCl present.

Comparative analysis between LIBS processing methods

Two methods were used to process LIBS data, and it is important to compare the results seen in the two to provide insight to the advantages and limitations of each. The methods applied to our data were univariate analysis and linear correlation between datasets, the methods for which were explained in chapter three. The advantage of the univariate analysis is obvious: it provides a simple number that is less convoluted to understand. There is no complexity to the simple numeric methodology applied for this analysis. This method does provide results, and we can see surface depletion of Cr. This technique does not tell us what factors change, only that the surface looks different than the unexposed sample, or the material seen deep within the sample. On the other hand, the numeric integration is able to look at elemental signals but requires much more work to normalize and correct than the linear correlation. When this method is used on multiple emission lines or datasets, more of the factors causing complexity that occludes the features of corrosion are made clear. For example, in figure 5-1 the Cr signal is normalized to the Cr signal seen in the unexposed sample. By doing this, we can reduce or eliminate concerns about changing parameters based on the formation of a hole in the sample and the changing plasma formation characteristics. The case where the two Cr emission lines are compared is not particularly useful, as the two lines have different intensities, meaning that the two do not result in the same intensity in the emission spectra.

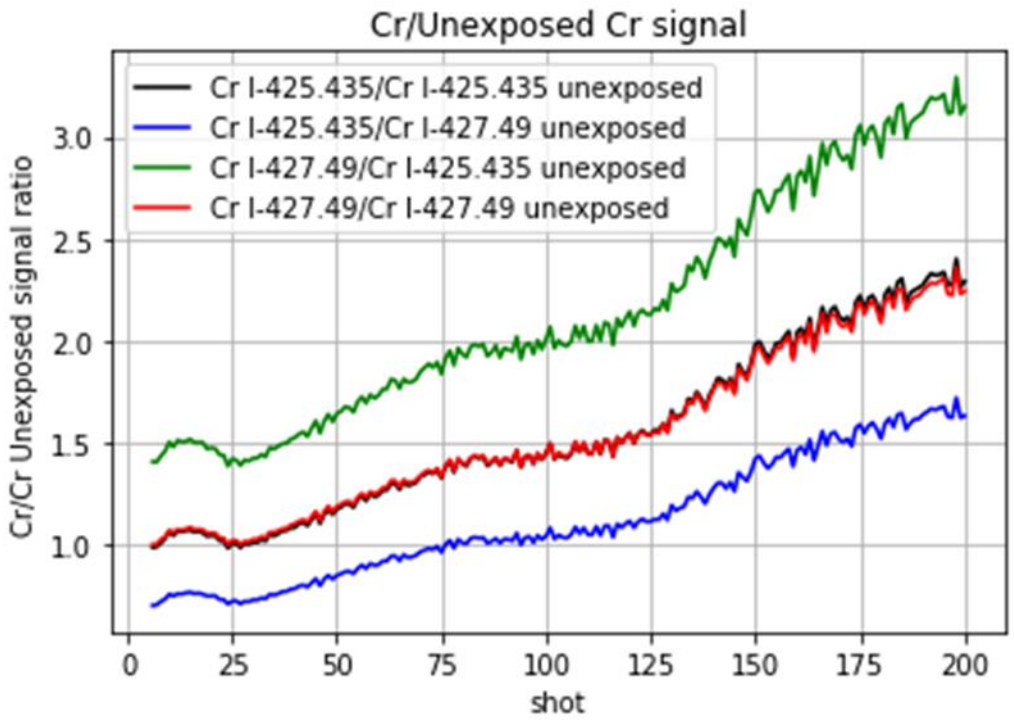

Figure 5-1: Cr signal normalized to unexposed sample for multiple wavelengths

This normalization should remove variation based on sample geometry changing with shot number. This was for the 2500 hr exposure.

Similarly, in figure 5-2 the Cr signal is normalized to the Ni signal from the same spectra, which should reduce or eliminate the variation associated with fluctuations in laser power. In this figure, we can see that there is a noticeable change in the signal around shot 50, corresponding to a depth of about 10 μm with the previously assumed ablation rate. This agrees with the EDS results that there are two regions of Cr content as a function of depth. It is plausible these are created from two physical processes, likely a near surface region where Cr is more easily reacted with salt, and a deeper section where diffusion of Cr controls the loss of Cr. In the EDS (shown in figure 4-3) we can see that these regions appear to have less depth dependence than what is seen in the LIBS results, implying that there may be some bias towards sensing the Cr emissions deeper into the sample.

Normalization can be done by dividing by the Ni signal of the same spectra to correct for variations in laser power, then dividing that signal by Cr signal normalized the same way from the unexposed sample to correct for the geometric efficiency of the LIBS process. The result is a signal that is corrected for both fluctuations in laser power and the changing geometry produced through the LIBS process. To re-iterate, in this methodology, the signal of a single Cr emission is compared to that of a Ni emission from the same spectra, and that signal is then compared to the signal of Cr normalized to Ni in the same way for the unexposed sample. This can be described as: $S = \frac{\frac{Cr_{exposed}}{Ni_{exposed}}}{\frac{Cr_{unexposed}}{Ni_{unexposed}}}$ This method should correct for errors produced by laser power, and those produced by changing geometry. The results from this method are shown in Figure 5-3. This figure is noticeably lacking the peak seen in some earlier figures around 24 shots from the changing focus of the laser. This profile is also less noisy in the shallow and medium depth ranges. There is moderate signal noise deep into the sample, similar to the other profiles. This depth profile attempts to correct for all the factors that could lead to an incorrect

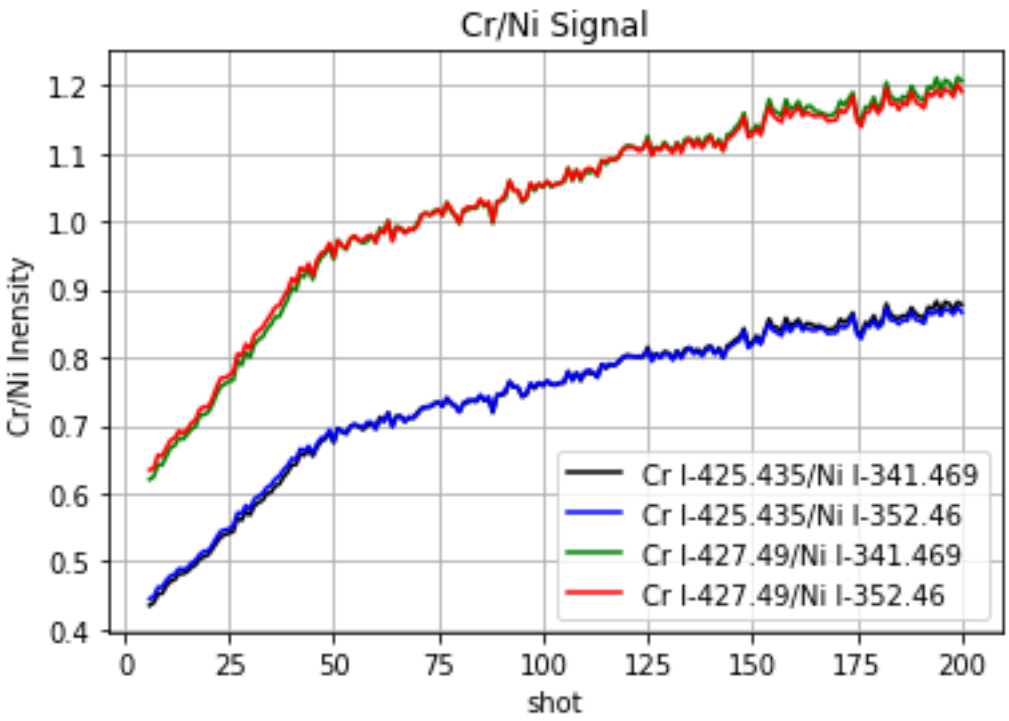

Figure 5-2: Cr signal normalized to the Ni from the same spectra

Cr signal normalized to the Ni signal from the same sample for multiple wavelengths based on the 2500 hr exposure to molten salt. This method of normalization should reduce the impact of laser power fluctuations on the dataset.

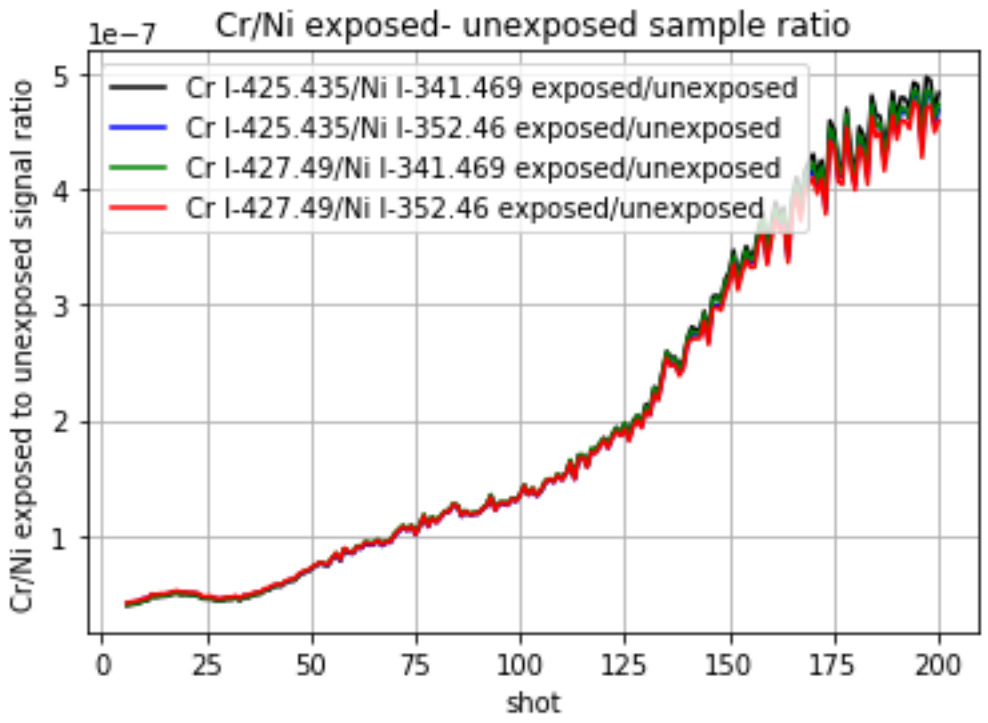

Figure 5-3: Cr signal normalized to both Ni from the same spectra and Cr from unexposed sample

This methodology should reduce fluctuations in laser power and the geometric variation of the data. This example was done with the 2500 hr exposure.

profile. Similar features are visible; there appears to be a few differing regions where Cr content varies with depth. In total, this correction seems to remove most features and leaves a signal that does not really explain much of the variation seen in EDS. This likely means that this data correction approach to eliminate systematic errors likely leads to removing some important information from the analysis.

The second method for analysis of the LIBS data was that of linear correlation between spectra. This method takes one spectrum, then evaluates how similar it is to another spectrum. This methodology was presented in [46], where they found it to be effective in identifying different layers of material, and showed that it reduced noise and complexity from the spectra. This methodology calculates a linear correlation between two spectra using the equation: $r = \frac{\sum_i (x_i - \bar{x})(y_i - \bar{y})}{\sqrt{\sum_i (x_i - \bar{x})^2}\sqrt{\sum_i (y_i - \bar{y})^2}}$ to find a value r that can be used to compare spectra. It is worth comparing unexposed samples to exposed samples this way, as well as surface and maximum ablation depth regions. These results are shown in figure 5-4. Shot 120 was used as a comparison, as at this depth material should be similar to bulk material. This figure allows for a much simpler method of studying the behavior of the sample and is important, as it is a much more rapid technique that can deliver similar information. This technique provides another way to look at the sample and see the general variance with depth. The advantage of this technique is that it provides a simple way to look at the sample that takes no calibration to find the similarity between spectra. This technique would show if something unexpected is happening, as if there were not good agreement for samples near each other, we would know something was wrong in the processing of data, or with the data itself. The results from both univariate analysis and linear correlation are plotted together in figure 5-5. In this way, we can see that there is very good agreement between the two, suggesting that the variation in the Cr explains most of the variation in the spectra as a function of depth. It appears that the univariate analysis captures more of the complexity of the data but has more noise in its results.

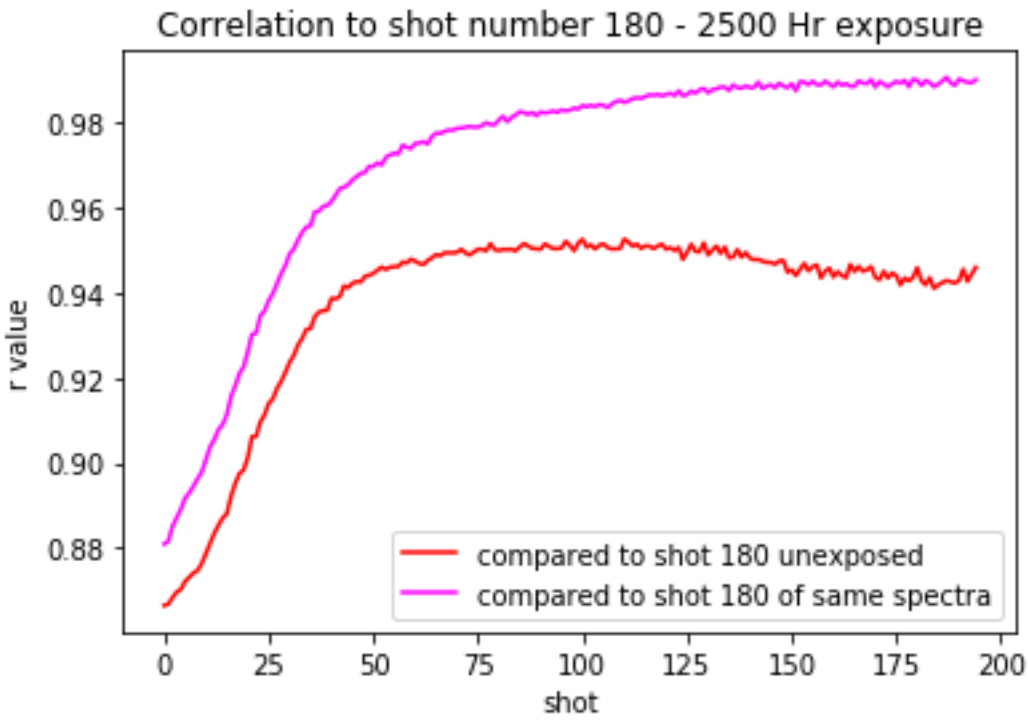

Figure 5-4: Linear correlation results

Linear Correlation comparing the spectra at significant depth to the spectra of that location in all 100 spots, and to the spectra seen in the unexposed sample. There is greater agreement with between the spectra gathered from the same sample than when comparing to the unexposed sample.

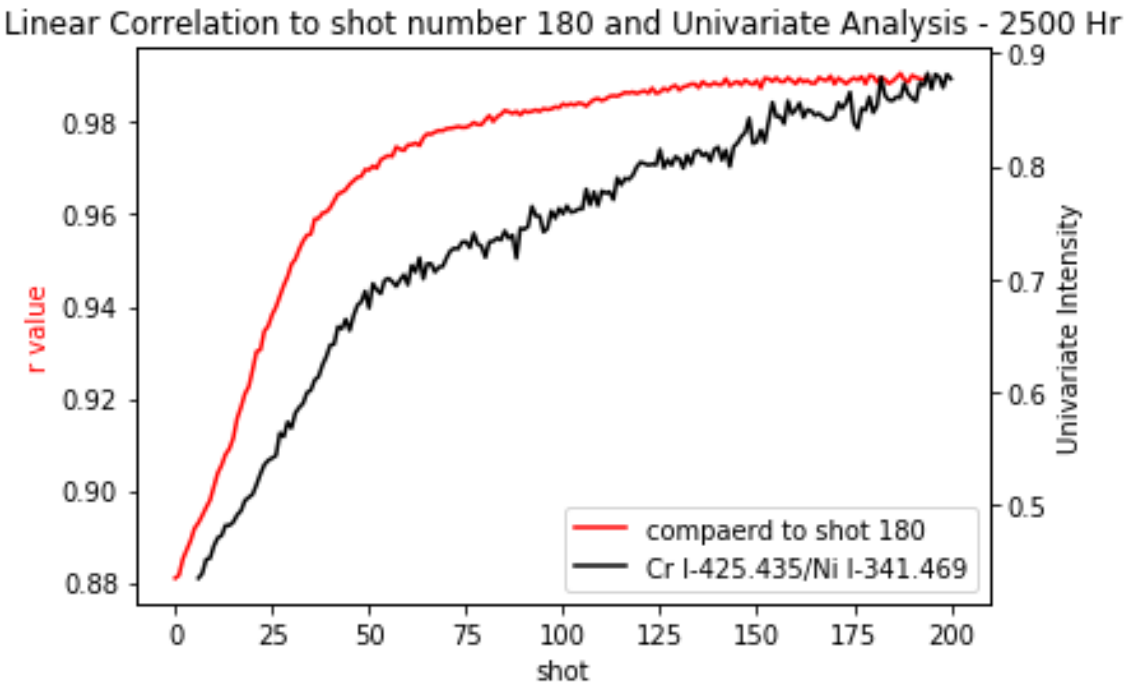

Figure 5-5: Linear correlation and normalized LIBS emission

Linear correlation and normalized Cr signal plotted together showing that the variance seen in the data is largely explained in the change seen in the Cr as a function of depth.

Comparative analysis to SEM

SEM and EDS data was taken for the 2000 and 2500 hr exposure samples. It is worth comparing the well accepted technique of SEM with LIBS to confirm LIBS is providing accurate insight on material behavior. Results from EDS were relatively clear, and showed consistency between samples. The samples both showed around 10% Cr at the salt-metal interface. The 2000 hour exposure has approximately 14% Cr content at the maximum depth EDS was taken, while the 2500 hour exposure resulted in 12% Cr at maximum depth of EDS. Original Cr content was 16%. Depths were comparable, around 20 μm, and SEM images with EDS linescan locations are shown in figure 5-6. Here we can see that there are two major regions of interest in the EDS profile: There is an initially rapid change in Cr content near the exposed surfaxce, and a slow change in Cr content further from the salt-metal interface at about 10 μm from the sample surface. In figure 5-7, the ablation rate estimate is adjusted to 0.12 microns per shot in order to better fit the EDS data. This should give us a better estimate of the ablation rate.

Reporting Variance in Signal

A useful addition is that of including the maximum, minimum and standard deviation of the signal seen for this work. If there is variation that is significant, it would lessen the impact of the work, and would make for less believable work. To that end, the maximum, minimum and standard deviations were calculated and reported in figure 5-8. In this we can see that while there is noise, the trends that we observe in surface depletion, and having rich material within the sample are on a significantly larger scale than the standard deviation, suggesting they are not just noise.

Estimating Ablation Depth

It has been mentioned several times that assuming a linear ablation rate for LIBS is not correct. To that end, an attempt was made to calculate the ablation rate using the

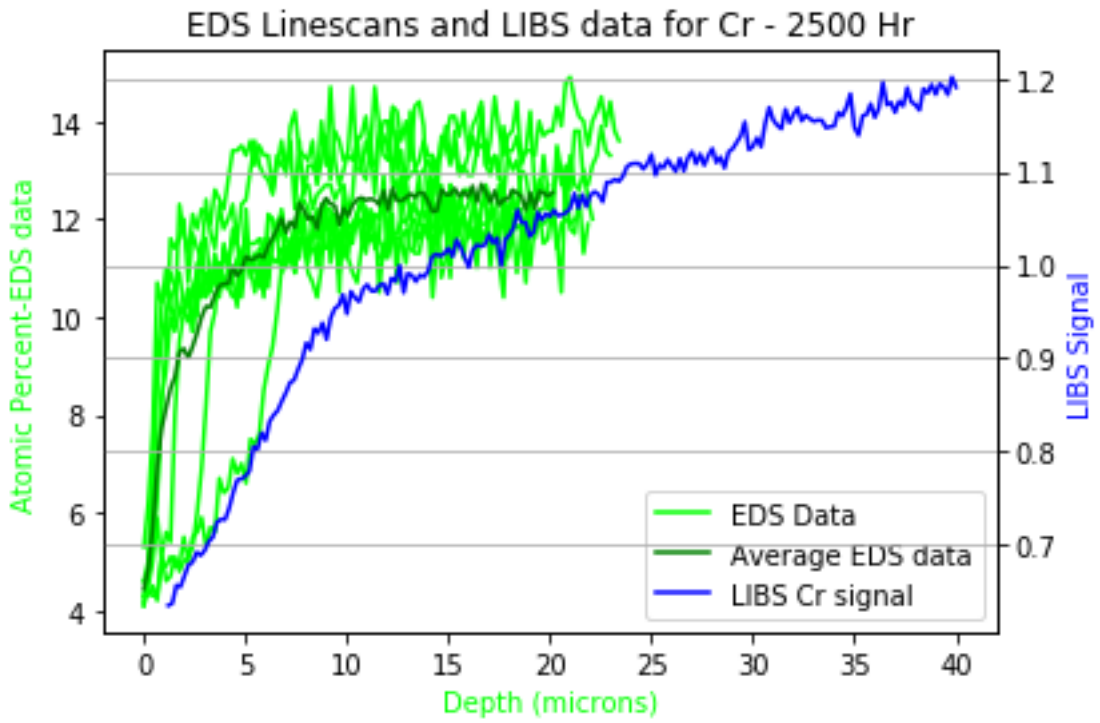

Figure 5-6: EDS data and LIBS with assumed .2 micron per shot ablation rate

With these signals plotted together, a similar shape of the plots are seen, however the LIBS appears to overestimate the depth to which it reaches. We can see that this fit does not make the LIBS and EDS fit together particularly well.

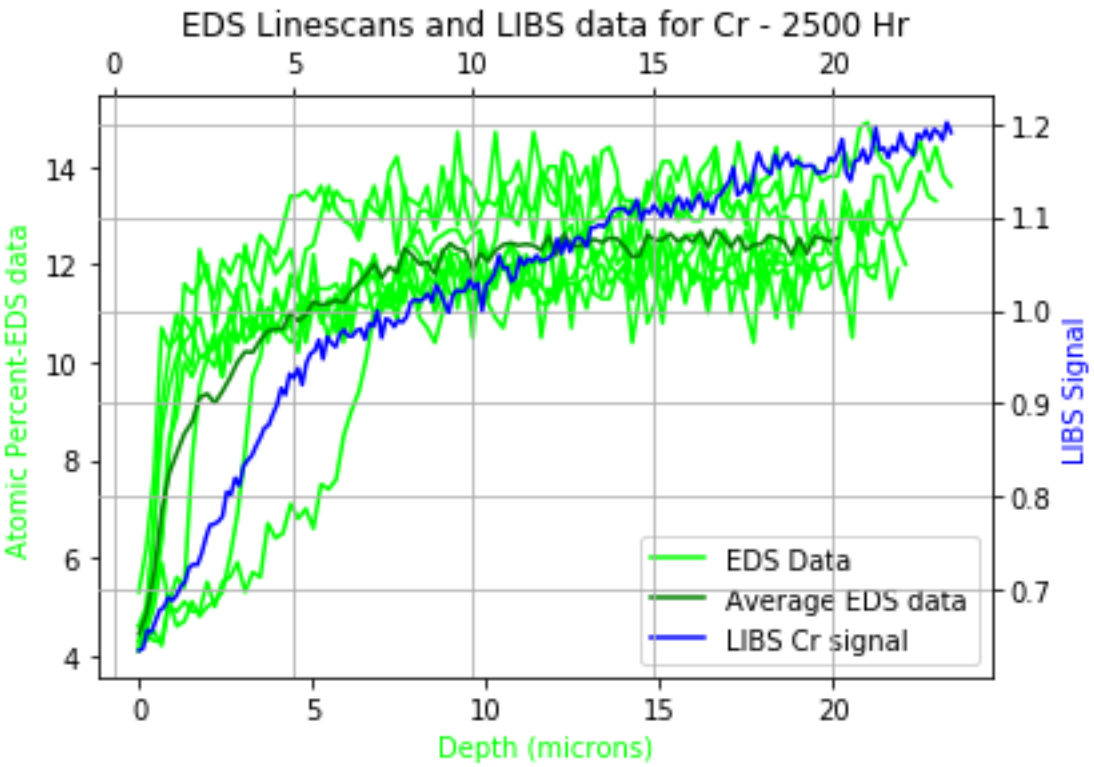

Figure 5-7: EDS and LIBS with new ablation rate estimate

EDS Linescans, their average and the average LIBS signal plotted together with a new fit estimating the average ablation rate as 0.12 microns per shot to better fit the LIBS profile to the EDS data.

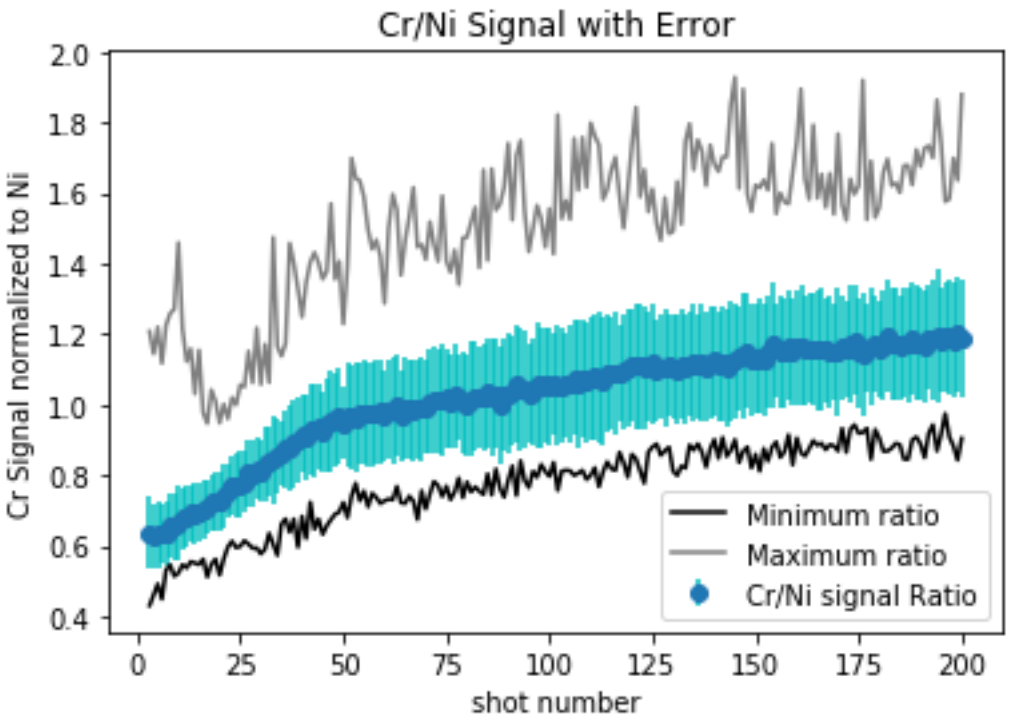

Figure 5-8: LIBS Linescans with maximum, minimum, and standard deviation reported to assist with understanding the variance of the technique.

methodology outlined in the Applied Physics A article from Agresti [47]. The relevant math is described in the appendix of this thesis. However it is worth reporting that they use a fitting parameter to consider several important physical parameters. This parameter (k) wraps the terms of the laser power, heat needed to make material in to plasma, and some length parameters into one single term. This term must have units of length to the fourth power to produce a length output. This term is not rigorously defined in the paper, and thus further explanation will not be made past what is needed to understand why it differs in our work from what was used in their work.

The k parameter was ~1500000 for the case presented in Agresti to fit the given spot size and depth occur. For our case, k is significantly lower. First, our power density was about half that of what was used in the Agresti paper. Secondly, copper, the material used in the paper describing this method [47], has a significantly lower heat of vaporization, heat of fusion, and melting point, all which contribute to being more quickly ablated. Thus a higher k parameter is expected compared to the Ni used in our work. For our work, without having a maximum crater depth, there is not a perfect way to estimate the appropriate k. However we can see the trends seen in EDS and LIBS appear to have most agreement with the k parameter about an order of magnitude lower than that used in the Agresti paper. Given this k, the ablation rate is relatively uniform, and the previous assumptions of a linear ablation rate will not be significantly revised. The corrected ablation rate is used in figure 5-9, where the same general trends emerge as before. It is also worth noting that even with the assumed k in the Agresti paper, the early spots within their study showed a relatively linear ablation rate.

Overall, the largest trend that is evident from the LIBS data is near-surface depletion of Cr following exposure to molten salt. The near-surface depletion of Cr was observed with LIBS, and confirmed with EDS. The comparison between the two suggests that LIBS does show similar trends as EDS, validating that LIBS is capable of detecting important depth-dependent chemical changes in exposed samples. In this work, some clear limitations and difficulties were seen with LIBS. First, LIBS requires that the processing

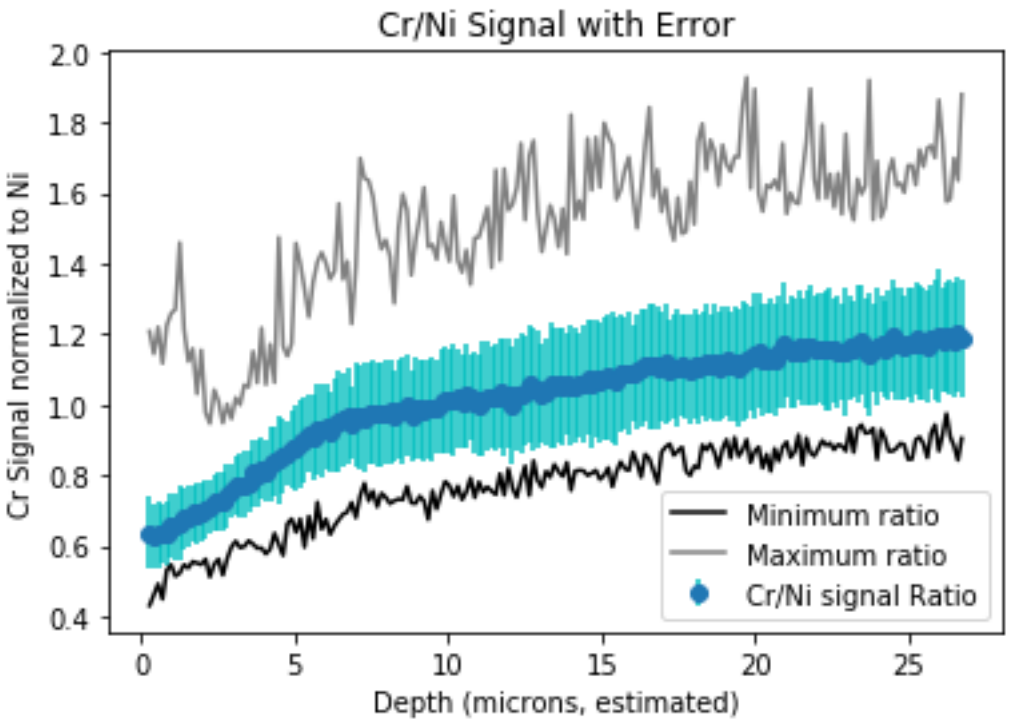

Figure 5-9: The same figure with error bars showing using the correction methodology discussed to estimate the real depth at which each shot occurs.

done by the instrument or that developed by the user after the fact is used. This differs from EDS where there is more trust in the instrument's included software to calculate the amount of a material present.

LIBS has some more complicated interactions than EDS; re-deposition of material, an emission that varies as a function of depth on a uniform sample, and lack of visibility of elements based on experimental conditions. In this work, it would have been great to be able to look for the presence of Cl, to confirm if the small amounts of elements that were left from salt were in the form salt trapped in surface features, or if those elements were present in some other form, metallic, intermetallic, or otherwise present outside of a salt. This was not possible for the reason mentioned in chapter 3 of the Ar cover gas having emissions that overlap with the Cl emission lines in the region of optical emissions observed by the instrument used. Future work could either use a different cover gas to avoid this problem, or could use a wider range spectrometer, allowing for studies of the optical spectrum where Cl and Ar do not have overlapping emissions. Much of the difficulty dealing with LIBS data is that of correcting for the depth dependent nature of the response seen. The signal produced in a single plasma creation event in a LIBS instrument is a function of several factors, the focus of the laser, the depth to which the material has been ablated, the shape of the laser power distribution, the width of the laser beam, and the depth to which it has penetrated all play significant roles in the way a LIBS signal varies. This complexity might be further studied to make sure that all results seen in this work are accurate, however these complexities are inherent to the technique. They might be confirmed to be absent, however they must be considered any time LIBS is conducted, meaning they likely could not be removed from a future study. A final area of further work would be changing the cover gas for this study. This would not be an overly difficult task, and likely would not change the core of the results. What might change the visibility of Cl in the emission spectra. By enabling the sampling of Cl, it is possible that that signal could be compared to the signals seen for Mg and K, which would determine if the small amounts of each present were the result of some complex chemistry or if this

was salt trapped at pores, cracks, or any surface feature. There are several interesting directions that further work on LIBS and molten salt that could be pursued.

With these complexities and further work, the benefits of LIBS are still likely worthwhile. Not needing to do sample preparation for studies and the ability to image anywhere an optical fiber can reach is a benefit that is of huge benefit for the ability to study ongoing corrosion. Molten salt reactors will require characterization of their behavior to ensure performance as designed: LIBS is a tool that can enable characterizing corrosion with limited access to a sample and without significantly damaging a specimen. For these reasons, LIBS is a technique that merits continued and further investigation.

CHAPTER SIX – CONCLUSIONS

MSRs are a vital technology if the world energy demand is to be met without relying on fossil fuels. They have the potential to provide a safe and efficient way to produce cheap, clean, and reliable electricity. Their long list of benefits including the usage of Th, the transmutation of waste, and the production of medical isotopes provide additional benefits that are needed. Enabling this technology requires understanding of the materials challenges faced, particularly corrosion. LIBS is an excellent tool for this purpose, as it can detect the loss of Cr or the least noble metal in the alloy. LIBS is a versatile and rapid data analysis tool that could be implemented on-site allowing for rapid characterization in a plant environment. For these reasons along with the performance demonstrated in this work, LIBS is a tool that should be considered for characterizing the system when a molten salt reactor is built. This would necessitate further development of the technique in experiments to provide further insight than in this work.

In this work, evidence has been presented comparing EDS and LIBS, and a case has been made that LIBS is able to see similar features as EDS for Cr and Ni. This suggests that for elements that EDS is capable of imaging, LIBS is valid and can provide the same information along with the benefit of improved measurement versatility (e.g., in-situ characterization). In addition, LIBS data and results were presented for the elements K, Mg and O, elements that EDS has difficulty detecting. Having shown LIBS to work for Cr and Ni should provide validation for these results that could not be achieved with EDS. Mg was found to be localized to the surface, and K was found in minute amounts. This and the presence of O everywhere Mg was found suggest that MgO was the predominant Mg compound on the samples, not salt. This is possibly a result of washing samples, exposing them to air and water which would allow $MgCl_2$ to form MgO and Cl_2. Of greater interest for molten salt reactors is that LIBS was able to examine the full range of depth to which Cr is depleted, and the obtained results matched the EDS results. The depletion of least noble metals is the primary method of corrosion in molten salt

systems, and LIBS being able to characterize this primary problem demonstrates that there is utility in the technique that would merit its consideration for monitoring of molten salt exposed systems. The limitations of LIBS, such as the ability to sense Cl in the presence of Ar cover gas for example, should be possible to overcome. Changing cover gas, using LIF and other secondary techniques provide the possibility of removing the limitations of seeing certain elements.

Future work on the topic of LIBS for molten salt corrosion would necessitate finding samples that had more evidence of salt-trapping or other unusual features. In those cases, LIBS would enable seeing features that would not be rapidly visible with EDS. It would be beneficial in addition to these to evaluate samples that had seen more complex chemical situations that might produce other effects of interest past simple depletion of the least noble metal from the sample.

REFERENCES

[1] M. W. Rosenthal, P. R. Kasten, and R. B. Briggs, "Molten-Salt Reactors—History, Status, and Potential," *Nuclear Applications and Technology,* vol. 8, no. 2, pp. 107-117, 1970/02/01 1970.

[2] W. B. Cotrell, "Reactor Program of the Aircaft Nuclear Propulsion Project," vol. ONRL-1234, ORNL, Ed., ed, June 1952.

[3] W. D. Manly *et al.*, "Aircraft Reactor Experiment- Metallurgical Aspects," vol. ORNL-TM-2349, ORNL, Ed., ed, Dec 1957.

[4] U. S. AEC, "An Evaluation of the Molten Salt Breeder Reactor," vol. Wash-1222, ed, Sept 1972.

[5] J. R. Keiser, "STATUS OF TELLURIUM-HASTELLOY N STUDIES I N MOLTEN FLUORIDE SALTS," vol. ORNL/TM-6002, ORNL, Ed., ed, Oct 1977.

[6] Victor Ignatiev *et al.*, "Intergranular tellurium cracking of nickel-based alloys in molten Li, Be, Th, U/F salt mixture," *Journal of Nuclear Materials,* vol. 440, no. 1-3, pp. 243-249, Sept 2019.

[7] H. E. McCoy, "Status of Materials Development for Molten Salt Reactors," vol. ONRL-TM-5920, ORNL, Ed., ed, 1978.

[8] H. E. McCoy, "An Evaluation of the Molten Salt Reactor Experiment Hastelloy N surveilance Specimens- First Group," vol. ORNL-TM-1997, ORNL, Ed., ed, 1967.

[9] H. E. McCoy, "An Evaluation of the Molten Salt Reactor Experiment Hastelloy N Surveillance Specimens- Second Group," vol. ORNL-TM-2359, ORNL, Ed., ed, 1969.

[10] H. E. McCoy, "An Evaluation of the Molten Salt Reactor Experiment Hastelloy N Surveillance Specimens- Third Group," vol. ONRL-TM-2647, ORNL, Ed., ed, 1970.

[11] H. E. McCoy, "An Evaluation of the Molten Salt Reactor Experiment Hastelloy N Surveillance Specimens- Fourth Group," vol. ORNL-TM-3063, ONRL, Ed., ed, 1971.

[12] R. C. Robertson, "MSRE Design and Operations Report Part I," vol. ORNL-TM-728, ONRL, Ed., ed, 1965.

[13] P. N. Haubenreich, J. R. Engel, B. E. Prince, and H. C. Claiborne, "MSRE Design and Operations Report Part III. Nuclear Analysis," vol. ORNL/TM-730, ORNL, Ed., ed, Feb 1964.

[14] W. R. Grimes, "Radiation Chemistry of MSR System," vol. ONRL-TM-500, ORNL, Ed., ed, Mar 1963.

[15] M. W. Rosenthal, P. N. Hauenreich, and R. B. Briggs, "The Development Status of Molten Salt Breeder Reactors," vol. ORNL-TM-4812, ORNL, Ed., ed, Aug 1972.

[16] "The Use of Thorium in Nuclear Power Reacotrs," vol. Wash 1097, ed, June 1969.

[17] W. R. Grimes, "Chemical Research and Development for Molten Salt Breeder Reactors," vol. ORNL-TM-1853, ORNL, Ed., ed, 1967.

[18] J. R. Keiser, "Compatabiliy Studies of Potential Molten Salt Breeder Reactor Materials in Molten Flouride Salts," ORNL, Ed., ed, May 1977.

[19] J. R. Engel, W. R. Grimes, H. F. Bauman, E. H. McCoy, J. F. Dearing, and W. A. Rhoades, "CONCEPTUAL DESIGN CHARACTERISTICS OF A DENATURED MOLTEN-SALT REACTOR WITH ONCE-THROUGH FUELING," vol. ONRL-TM-7207, ORNL, Ed., ed, July 1980.

[20] D. F. Williams, "Assessment of Candidate Molten Salt Coolants for the Advanced High-Tmpererature Reactor (AHTR)," vol. ORNL-TM-2006/12, ORNL, Ed., ed, Mar 2006.

[21] L. R. Greenwood, "A new calculation of thermal neutron damage and helium production in nickel," *Journal of Nuclear Materials,* vol. 115, no. 2-3, pp. 137-142, April 1983.

[22] J. R. Keiser, J. H. DeVan, and D. L. Manning, "The Corrosion Resistance of 316 Stainless Steel to Li2BeF4," vol. ORNL-TM-5782, ORNL, Ed., ed, 1977.

[23] Shaoqiang Guo, Jinsuo Zhang, Wei Wu, and W. Zhou, "Corrosion in the Molten Fluoride and Chloride Salts for Nuclear Applications," *Progress in Materials Science,* no. 97, pp. 448-487, 2018.

[24] C. F. Baes, "The chemistry and thermodynamics of molten salt reactor fuels," *Journal of Nuclear Materials,* vol. 51, no. 1, pp. 149-162, May 1974.

[25] S. S. Raiman, "Aggregation and data analysis of corrosion studies in molten chloride and fluoride salts," *Journal of Nuclear Materials,* 2018.

[26] F.-Y. Ouyang, "Effect of moisture on corrosion of Ni-based alloys in molten alkali fluoride FLiNaK salt environments," *Journal of Nuclear Materials,* vol. 437, no. 1-3, pp. 201-207, 2013.

[27] F.-Y. Ouyang, "Long-term corrosion behaviors of Hastelloy-N and Hastelloy-B3 in moisture-containing molten FLiNaK salt environments," *Journal of Nuclear Materials,* vol. 446, pp. 81-89, 2014.

[28] D. E. Holcomb, G. F. Flanagan, B. W. Patton, J. C. Gehin, R. L. Howard, and T. J. Harrison, "Fast Spectrum Molten Salt Reactor Options," vol. ORNL/TM-2011/105, ORNL, Ed., ed, July 2011.

[29] Bruce Pint, Jake W. McMurray, Stephen S. Raiman, James M. Kurley III, William S. Ponder, and D. Sulejmanovic, "Corrosion of 316H Stainless Steel in Molten NaCl-MgCl2 With and Without Mg as a Redox Control Additive," ORNL, Ed., ed, Aug 2019.

[30] D. Olander, "Redox condition in molten fluoride salts: Definition and control," *Journal of Nuclear Materials,* pp. 270-272, Feb 2002.

[31] Masatoshi Kondo *et al.*, "Metallurgical study on corrosion of austenitic steels in molten salt LiF–BeF2 (Flibe)," *Journal of Nuclear Materials,* vol. 386-388, pp. 685-688, Apr 2009.

[32] Luke Olson, Kumar Sridharan, Mark Anderson, and T. Allen, "Nickel-plating for active metal dissolution resistance in molten fluoride salts," *Journal of Nuclear Materials,* vol. 411, no. 1-3, pp. 51-59, Apr 2011.

[33] E.-Y. Choi, "Feasibility tests of nickel as a containment material of molten Li2O-LiCl salt containing Li metal at 650 °C during electrolytic reduction," *Journal of Nuclear Materials,* vol. 495, pp. 85-90, 2017.

[34] J. R. Keiser, J. H. DeVan, and E. J. Lawrence, "Compatibility of molten salts with type 316 stainless steel and lithium," *Journal of Nuclear Materials,* vol. 85-86, pp. 295-298, Dec 1979.

[35] J. W. Koger, "EVALUATION OF HASTELLOY N ALLOYS AFTER NINE YEARS EXPOSURE TO BOTH A MOLTEN FLUORIDE SALT AND AIR AT TEMPERATURES FROM 700 TO 560°C," vol. ORNL-TM-4189, ORNL, Ed., ed, Dec 1972.

[36] V. Ignatiev, "Alloys compatibility in molten salt fluorides: Kurchatov Institute related experience," *Journal of Nuclear Materials,* vol. 441, no. 1-3, pp. 592-603, 2013.

[37] W. R. Huntley and M. D. Silverman, "System Design Description of Forced-Convection Molten-Salt Corrosion Loops MSR-FCL-3 and MSR-FCL-4," vol. ORNL-TM-5540, ORNL, Ed., ed, Nov 1976.

[38] NIST. Atomic Spectra Database [Online].

[39] A. Bengtson, "Laser Induced Breakdown Spectroscopy compared with conventional plasma optical emission techniques for the analysis of metals – A review of applications and analytical performance," *Spectrochimica Acta Part B,* vol. 134, pp. 123-132, 2017.

[40] S. P. Ammon Williams, "Laser-Induced Breakdown Spectroscopy (LIBS) Measurement of Uranium in Molten Salt," *Applied Spectroscopy,* vol. 72, pp. 1029-1039, June 18, 2018.

[41] Arel Weisberg, Rollin E. Lakis , Michael F. Simpson, Leo Horowitz, and J. Craparo, "Measuring Lanthanide Concentrations in Molten Salt Using Laser-Induced Breakdown Spectroscopy (LIBS)," *Applied Spectroscopy,* vol. 68, p. 937, Sept. 1 2014.

[42] Samuel Moncayo *et al.*, "Exploration of megapixel hyperspectral LIBS images using principal component analysis," *journal of Analytical Atomic Spectrometry,* vol. 33, pp. 210-220, 2018.

[43] B. A. Pint *et al.*, "Re-establishing the paradigm for evaluating halide salt compatibility to study commercial chloride salts at 600°C–800°C," vol. 70, no. 8, pp. 1439-1449, 2019.

[44] Richard T. Mayes *et al.*, "Purification of Chloride Salts for Concentrated Solar Power Applications," vol. ORNL/LTR-2018/1052, ORNL, Ed., ed, 2018.

[45] Stephen S. Raiman, Richard T. Mayes, J. Matt Kurley, Riley Parrish, and E. Vogli, "Amorphous and partially-amorphous metal coatings for corrosion resistance in molten chloride salt," *Solar Energy Materials and Solar Cells,* vol. 201, 2019.

[46] M. P. Mateo, G. Nicolas, V. Pinon, and A. Yanez, "Improvements in depth-profiling of thick samples by laser-induced breakdown spectroscopy using linear correlation," *SURFACE AND INTERFACE ANALYSIS,* vol. 38, pp. 941-948, 2006.

[47] Juri Agresti and S. Siano, "Depth-dependent calibration for quantitative elemental depth profiling of copper alloys using laser-induced plasma spectroscopy," *Applied Physics A,* no. 117, p. 4, 2014.

APPENDIX

Below are the equations used in chapter 5 to iteratively calculate the ablation rate as a function of depth. This begins with attempting to solve for z_b at one shot, needing to find $\Delta z_b(1)$ to then find $z_b(1)$. This process is then iterated to find $z_b(N)$. These equations are laid out in the Agresti paper[47] but are more thoroughly detailed in their solution here. An additional equation is the radial power distribution, $E_i(r)$ describing the beam characteristics of the laser used in this work.

$$h(r) = k\frac{Ei(r)}{S(zb)}cos(\theta(r)) \qquad \Delta z(r) = \frac{h(r)}{cos(\theta(r))}$$

$$\Delta V = 2\pi\int_0^R r\Delta z(r)dr \qquad \Delta z_b = \frac{\Delta V}{\frac{dV}{dz_b}}$$

$$z_b(N+1) = z_b(N) + \Delta z_b(N)$$

$$V_P(zb) = \frac{\pi}{2}z_b R^2$$

$$z_b(N+1) = z_b(N) + \Delta z_b(N)$$

$$z_b(0) = 0, \qquad z_b(1) = 0 + \Delta z_b(1)$$

$$E_i(r) = \frac{1}{\sigma\sqrt{2\pi}}e^{-\frac{1}{2}\left(\frac{r-\mu}{\sigma\sqrt{2}}\right)^2} \quad \sigma = \frac{R}{2} \qquad \mu = 0$$

$$E_i(r) = \frac{\sqrt{2}}{R\sqrt{\pi}}e^{-\frac{1}{2}\left(\frac{r\sqrt{2}}{R}\right)^2}$$

$$\Delta z_b(1) = \frac{\Delta V}{\frac{dV}{dz_b}} = \frac{2\pi\int_0^R r\Delta z(r)dr}{\frac{\pi}{2}R^2} = \frac{4}{R^2} * \int_0^R r\frac{k\frac{Ei(r)}{S(zb)}cos(\theta(r))}{cos(\theta(r))}dr$$

$$= \frac{4}{R^2} * \int_0^R r\frac{k\frac{Ei(r)}{S(zb)}cos(\theta(r))}{cos(\theta(r))}dr = \frac{4}{R^2} * \int_0^R rk\frac{Ei(r)}{S(zb)}dr$$

$$= \frac{4\,k}{R^2 S(z_b)} * \int_0^R r * Ei(r) * dr = \frac{4\,k}{R^2 S(z_b)} * \frac{\sqrt{2}}{R\sqrt{\pi}} * \frac{(e-1)R^2}{2e}$$

$$\Delta z_b = \frac{2\sqrt{2}\,k}{\sqrt{\pi}\,R * S(z_b)} * \frac{(e-1)}{e}$$

$$S(0) = \pi R^2$$

$$S(z_b) = \frac{\frac{\pi}{6}R}{z_b^2}\left[(R^2 + 4Z_b^2)^{\frac{3}{2}} - R^3\right]$$

VITA

William Stephen Ponder was born March 25, 1996 to LtC Stephen Eric Ponder and MaryKay Ponder in Sierra Vista, AZ. William grew up there with his younger brother, Stephen Fredrick Ponder. His grandmother lived with them for several years before her passing and was an influence towards advanced education. William Ponder earned the Eagle Scout award in July of 2010. He graduated as the Valedictorian of Buena High School Class of 2014. He attended The University of Tennessee Knoxville beginning in the fall of 2014 studying nuclear engineering. During his time at UTK, he served as vice president and then president of the UTK Clay Target Team. He earned recognition as a collegiate all American through the National Skeet Shooting Association. He Graduated with his Bachelors of Science in Nuclear Engineering in May of 2018. Following this, he enrolled as a PhD student working for Steve Zinkle at UTK with assistance and mentorship from Stephen Raiman and Kristian Myhre at Oak Ridge National Laboratory.